Escola Tècnica Superior d'Enginyeria de Telecomunicació de Barcelona

UNIVERSITAT POLITÈCNICA DE CATALUNYA

Master Thesis

Design and Performance Analysis of Switched Beam Series-Fed Patch Antenna Array for 60 GHz WPAN Applications

Rabia Zainab Syeda

Director:

Prof. Jordi Romeu Robert

Name: **Rabia Zainab Syeda**

Thesis Title: **Design and Performance Analysis of Switched Beam Series-Fed Patch Antenna Array for 60 GHz WPAN Application**

Thesis Director: Prof. Jordi Romeu Robert

Academic Year: 2014

Department of Signal Theory and Communications (TSC)

Polytechnic University of Cataluña (UPC)

Abstract

This project gives a detailed study of the Design and Performance analysis of series fed patch antenna array for 60 GHz system applications. The patch array designed in this project will act as an active element and can be used as the feed antenna of the dielectric flat lens antenna which is highly directive at 60 GHz. CPW (Coplanar Waveguide) is used as the feeding technique of the antenna array because it has lower transmission loss, lower profile especially on high frequency band. The purpose of the array is to perform the beam scanning with the shift in the frequency over the complete range of V-Band i.e. 57 GHz to 64 GHz.

The designs are simulated in HFSS which is a high frequency simulator for designing such antennas. Due to the low profile and small weight of these antennas, they are constructed in microstrip technology which allows easy integration with printed circuits. For the fabrication of antennas Laser machine LPKF and photolithographic process are used.

Acknowledgement

First of all thanks to Allah Almighty for His Blessings; my parents, my family and my friends for giving me moral support despite being so far.

I want to thank Prof. Jordi Romeu for giving me the opportunity to do this project, for his timely suggestions, guidance and for helping me out whenever I got stuck in my project. Special thanks to Marc Imbert for his never ending support in all the phases of the project. If it wasn't for him, this project would not have been completed in time. Thanks Marc for your patience, help, guidance and unconditional support in the development of the technical aspects of the project.

Last, I would like to thank Prof. Sebastian Blanch for helping me out in the measurement of the antenna in the Antenna Lab.

Contents

List of Figures:

List of Tables

1. Introduction

The purpose of this research is to design a CPW (coplanar waveguide) Series-fed Microstrip patch antenna Switched Beam array in 60 GHz band for WPAN applications. The Microstrip technology has been adopted in this project to benefit from the low-profile and low weight antenna configurations. CPW (Coplanar Waveguide) has been widely used in Microstrip patch antenna recently, compared with the microstrip feed line as it has lower transmission loss, lower profile especially on high frequency band. Moreover, in this project frequency dependent beam tilting method is used for arrays. They have advantage over phased arrays since they have multiple fixed beams which can be easily selected and implemented is far easier.

1.1 State of the Art: 60 GHZ MMIC for Wireless Technology

Millimeter-wave (mmW) technology for the 60-GHz band is one of the most exciting opportunities for circuit, antenna, and communication system engineers over the next decade. 60 GHz is, in fact, the beginning of a trend of escalating carrier frequencies that will deliver unprecedented data rates, several tens of gigabits per second, allowing uncompressed high-definition media transfers, sensing and radar applications, and virtually instantaneous access to massive libraries of information. Consumer demand for these applications will result in millions of 60-GHz communication devices produced and sold by 2015 [1-1].

The millimeter-wave band, especially the unlicensed spectrum at the 60 GHz carrier frequency, is at the spectral frontier of high-bandwidth commercial wireless communication systems. Compared with microwave band communication, spectrum at 60 GHz is plentiful (frequencies of 57–64 GHz are available in North America and Korea, 59–66 GHz in Europe and Japan), but attenuation is more severe (20 dB larger free space path loss due to the order of magnitude increase in carrier frequency, 5–30 dB/km due to atmospheric conditions, and higher loss in common building materials). These characteristics make 60 GHz communication most suitable for close-range applications of gigabit wireless data transfer [1-2].

In addition to providing massive bandwidth for future WPANs and WLANs, adoption of wireless connectivity will soon be necessary, which is evident from the consideration of skin and proximity effects, substrate losses, and dispersion of wired interconnects at carrier frequencies of 60 GHz to hundreds of GHz[1-2]. There have been an early market success for the portable reading and data access devices such as Amazon Kindle and Apples IPad. However the future of these infrastructures include the replacement of books, paper media, computer hard drives and as well as magnetic media by the cloud or other data repositories which are extremely inexpensive to fabricate. Fig .1 (adapted from [1-3]) shows the future office where the main paper and magnetic storage media will be replaced by the very high broadband wireless connectivity.

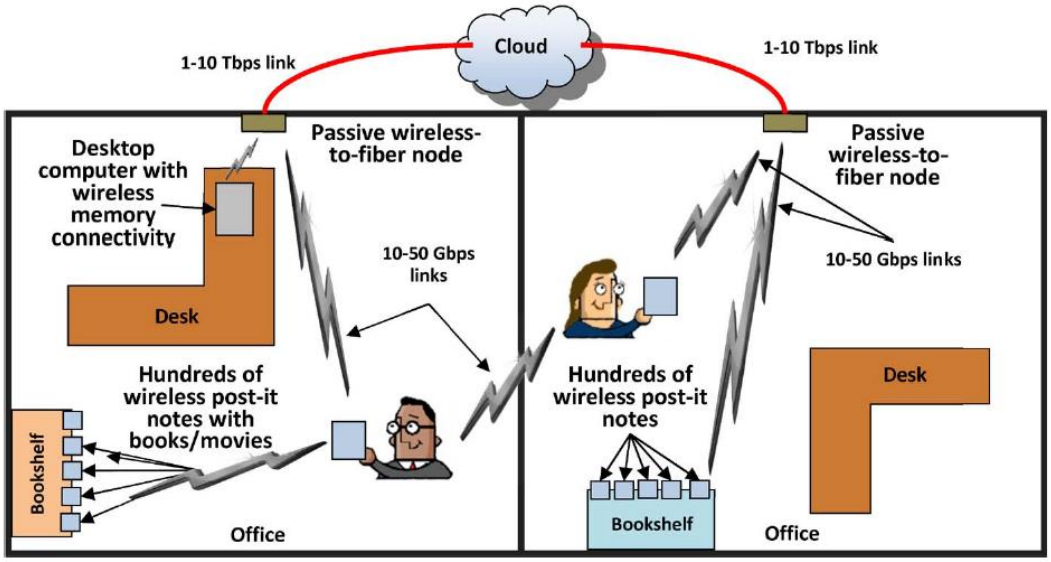

Fig. 1.1: Future of portable and inexpensive mm-Wave wireless devices that will cause the replacement of paper and magnetic storage media by the broadband wireless connectivity [1-3].

1.2 Challenges

1.2.1 Antennas

60 GHz chipsets exploit the short-carrier wavelength by incorporating antennas or antenna arrays directly on-chip or in-package. For the simplest and lowest-cost solutions, single antennas are attractive. Single-antenna solutions, however, must overcome the challenges of low on-chip efficiencies (typically 10% or less) and in-package antennas must overcome lossy package interconnects (standard wire-bonds are limited to under 20 GHz) [1-3].

1.2.2 Highly Integrated Tx and Rx for 60 GHz

The mm-scale wavelength of 60 GHz (5 mm in free space, and smaller on semiconductors and substrates having permittivity greater than 1.0) allows unprecedented levels of integration of analog and microwave components such as transmission lines and disparate monolithic microwave integrated circuits (MMICs) onto a single chip or package [1-3].

1.2.3 Modulation and Equalization

Digital communications at 60 GHz provides unique design trade-offs due to millimeter-wave hardware limitations and channel propagation characteristics. The wide operating bandwidth results in tight digital processing constraints and severe frequency-selective signal distortion known as inter symbol interference (ISI). Millimeter-wave modulation must also consider the increased presence of phase noise relative to microwave frequencies and limited output power, which makes nonlinear operation attractive [1-2].

1.3 60 GHz Standards

There are many standardization and commercialization efforts currently underway by the engineering community for 60-GHz WPAN. Current technical standards activities include IEEE 802.15.3c, WirelessHD, IEEE 802.11ad, the WiGig standard, and ECMA 387. All of these standards target short range 60-GHz networks. Table. 1 illustrates Major 60 GHz standards that are under development or modification.

Name	Maximum Data Rate (Gbps)		Application
	OFDM	SC	
WirelessHD	4	-	Uncompressed HD video
ECMA-387	4.032	6.35	Bulk Data Transfer and HD streaming
802.15.3c(TG3c)	5.7	5.2	Portable P2P file transfer and streaming
802.15.3c(TGad)	>1		Wireless Display, Rapid upload/download
WiGig	>7		File transfers, wireless display and docking and streaming high definition

Table. 1.1: Major 60 GHz Standards that are under development (data taken from [1-3])

1.4 Objectives

In this project, the aim is to design a patch antenna array which acts as active element and can be used as the feed antenna of the dielectric flat lens presented in [1-4]. For that purpose, patch antenna has been designed using the microstrip technology to operate at 60GHz with the bandwidth from 57GHz to 64GHz. CPW feeding technique has been used to excite the antenna. Later using this antenna, an array has been designed to operate in the frequency band of 57 GHz-64 GHz. The purpose of the array is to perform the beam scanning with the shift in the frequency so that the array has the scanning capabilities with the fixed multiple beams which can be selected individually and is used as the feeding array of the dielectric lens in [1-4].

1.5 Organization of Thesis

The complete thesis report is divided into 6 chapters. Following is the brief summary of each chapter

Chapter 1: Introduction

This chapter presents the motivation behind the thesis and general background of the 60 GHz WPAN technology. Also its list down the objectives that are to be full filled in the following project report.

Chapter 2: Antenna Parameters and Antenna Arrays

This chapter firsts explains the basic concepts of antennas and describes the parameters that are essential to understand while working of antennas. It also highlights the specific parameters associated

with the 60 GHZ integrated circuits. At the end this chapter deals with the concepts of antenna arrays and the design considerations and feeding networks for antenna

Chapter 3: Microstrip Patch antenna and CPW

This chapter gives an insight on why the microstrip technology is useful and what are the analysis methods, pros and cons and the feeding techniques of microstrip antennas. At the end this chapter also deals with the coplanar waveguide and its pros and cons.

Chapter 4: CPW Fed Microstrip Patch antenna Design and Results

This chapter gives the detail analyses of the work done in this thesis for the design of single patch antenna wit CPW feed both in simulation and in hardware. This chapter also explains the Cascade Microtech measurement system that is being used for measurement of S11 Parameters. All the results for single patch at 60 GHZ has been shown in this chapter.

Chapter 5: Series-Fed Linear Patch Antenna Array Design and Results

This chapter includes the design and simulation of the Series-fed linear array that has been the final goal of this project. This chapter describes in detail the measurement system build in the Antenna Lab of UPC for the 60 GHz measurements. All the results from the array prototypes are shown in this chapter.

References

1-1 R. Merritt, B60 GHz groups face off in Beijing over Wi-Fi's future, EE Times, May 18, 2010, accessed on May 31, 2010.

1-2 "60GHz Wireless: Up close and personal." Robert C. Daniels, James N. Murdock, Theodore S. Rappaport, and Robert W. Heath, Jr. , IEEE Microwave Magazine, December 2010 Supplement

1-3 "State of the Art in 60-GHz Integrated Circuits and Systems for Wireless Communications, T.S. Rappaport, J.N. Murdock, and F. Gutierrez, " Proceedings of the IEEE, vol.99, no.8, pp.1390-1436, Aug. 2011.

1-4 "Design of a Dielectric Flat Lens Antenna For 60GHz WPAN Applications", M.Imbert, J. Romeu and L. Jofre, Department of Signal Theory and Communication, Universitat Plitecnica de Catalunya.

2. Literature Review: Antenna Parameters and Antenna Array Concepts

In this chapter basic concept of antenna and some critical antenna performance parameters are being discussed. Also, the performance analysis of an antenna array is also being performed at the end.

2.1 Introduction

Antennas are metallic structures that radiate or receive electromagnetic waves. Antennas can be seen as the transition structure between transmission line and free space. According to IEEE definition of antenna, “Antenna is that part of transmitting or receiving system that radiate or receive radio waves” [2-1].

2.2 Antenna Parameters

The antenna performance can be gauged from a number of parameters. Certain critical parameters as discussed below:

2.2.1 Radiation Pattern

The radiation pattern of an antenna is the plot of the far field radiation as a function of spatial coordinates which are elevation angle θ and azimuthal angle φ. It is basically the plot of the radiated power of antenna. An isotropic antenna is the one that radiates equally in all directions. An isotropic antenna is not possible to realize in practice and is useful only for comparison purposes. A more practical type is the directional antenna which radiates more power in some directions and less power in other directions (fig 2.1).

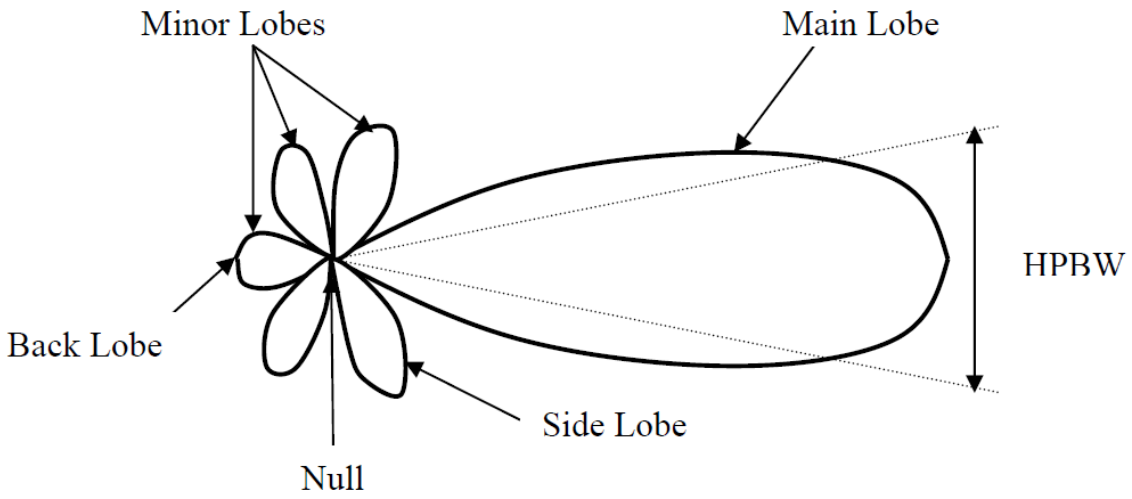

Fig 2.1: Radiation pattern of a generic directional antenna

The radiation pattern can be displayed with a 3D representation; but is common to show it in sections that follow the meridians (constant ϕ) or parallels (constant θ). These sections can be represented in

polar diagram that provides clearer information about the distribution of power in different spatial directions, or Cartesian coordinates that allow us to see important details in antennas with high values of directivity.

2.2.2 Radiation Power Density

The quantity that describes the power of electromagnetic waves is known as Poynting vector: [2-1]

$$W = E * H$$

W = instantaneous Poynting Vector (W/m2)

E = instantaneous Electrical field intensity (V/m)

H = instantaneous Magnetic field intensity (A/m)

The Poynting vector is power density and the total power crossing over a closed surface is obtained by integrating the Poynting vector over the closed surface given as:

$$P = \oiint W.ds$$

Where P = instantaneous total power (Watts)

2.2.3 Radiation intensity

Radiation intensity U of antenna is power radiated per unit angle [2-1]. Its units are watts per steradian. This parameter, in large distances, has the property of being independent of the distance. It is related to the radiated power density as follows:

$$U = r^2 W$$

2.2.4 Directivity and Gain

According to IEEE Standard Definition for Terms for antennas, directivity is the ratio of the radiation intensity of an antenna in a given direction and the radiation intensity averaged over all directions [2-2].

$$D = \frac{U}{Uo} = \frac{4\pi r U}{Prad}$$

D = Directivity (dimensionless)

Prad = Total radiated power (Watts)

The directivity of an antenna can be easily estimated from the radiation pattern of the antenna. An antenna that has a narrow main lobe would have better directivity, then the one which has a broad main lobe, hence it is more directive.

Another important performance parameter of antenna is its gain. Though it is quite similar to directivity of antenna but unlike directivity it takes into account of the efficiency of antenna and its directional capabilities.

Absolute Gain of an antenna is defines as “the ratio of radiation intensity of the antenna to the radiation intensity that is obtained by the input power to the antenna.” [2-1]

$$G = \frac{4\pi r U}{Pin}$$

Where Pin is the input power to the antenna.

2.2.5 Input Impedance

The input impedance of an antenna is defined by [2-1] as “the impedance presented by an antenna at its terminals or the ratio of the voltage to the current at the pair of terminals or the ratio of the appropriate components of the electric to magnetic fields at a point”. Hence the impedance of the antenna can be written as:

$$Zin = Rin + jXin$$

Zin = the antenna impedance at the terminals

Rin = the antenna resistance at the terminals

Xin = the antenna reactance at the terminals

The imaginary part, Xin of the input impedance represents the power stored in the near field of the antenna. The resistive part, Rin of the input impedance consists of two components, the radiation resistance Rr and the loss resistance Rl. The power associated with the radiation resistance is the power actually radiated by the antenna, while the power dissipated in the loss resistance is lost as heat in the antenna itself due to dielectric or conducting losses.

2.2.6 Return Loss

If the antenna is not perfectly matched to the transmission line and the generator than the electromagnetic waves are reflected back from the antenna and form the standing wave ratio. The quantity that describes the amount of the power that is reflected back is known as reflection coefficient Γ.

The Return Loss (RL) is however a parameter that indicates the amount of power that is “lost” to the load (antenna) and returns back as a reflection. Hence the RL is a parameter similar to the reflection coefficient to indicate how well the matching between the transmitter and antenna has taken place. The RL is given as by

$$RL = -20\log(\Gamma)$$

For perfect matching between the transmitter and the antenna, Γ = 0 and RL = ∞ which means no power would be reflected back, whereas a Γ = 1 has a RL = 0 dB, which implies that all incident power is reflected. For practical applications, a VSWR of 2 is acceptable, since this corresponds to a RL of -9.54 dB

2.2.7 Antenna Efficiency/Radiation Efficiency

The total antenna efficiency takes into account the ohmic losses of the antenna through the dielectric material, conduction losses, the reflective losses at the input terminals and losses within the structure of the antenna.

$$e_o = e_r e_c e_d$$

Where:

e_o = Total antenna efficiency (dimensionless)

e_r = Reflection efficiency = $(1-|\Gamma|^2)$ (dimensionless)

e_c = Conduction efficiency (dimensionless)

e_d = Dielectric efficiency (dimensionless)

2.2.8 Antenna Bandwidth

The antenna bandwidth is defined as the "range of frequencies with in which the antenna conform to the specific standard with respect to some characteristics" [2-1]. The antenna characteristics that are used to determine the bandwidth can be input impedance, radiation pattern Beamwidth polarization, side lobe level or gain. The bandwidth of a broadband antenna can be defined as the ratio of the upper to lower frequencies of acceptable operation.

$$BW_{broadband} = \frac{f_H}{f_L}$$

The bandwidth of a narrowband antenna can be defined as the percentage of the frequency difference over the center frequency.

$$BW_{narrowbamd}\ (\%) = [\frac{f_H - f_L}{f_C}] * 100$$

f_H = upper frequency

f_L = lower frequency

f_C = center frequency

One method of judging how efficiently an antenna is operating over the required range of frequencies is by measuring its VSWR or RL. A RL ≤ $-10dB)$ ensures good performance [2-1].

2.3 Antenna for 60 GHz Integrated Circuits

Designing and fabricating antennas at 60 GHz frequency (with size of the order of few microns) has been a challenge due to the small distance between the radiating elements, surrounding metal layers and substrate. The radiation losses and conduction losses are extremely large due to substrate absorption and conduction currents thus these antennas have very high losses and very low gains. However the removal of all the connections between the RF circuits and the antennas causes a substantial decrease in cost and eases the manufacturing processes of the antennas. [2-3]

According to [2-3], the effective wavelength at 60 GHz for an IC substrate is estimated by using the frequency and material properties of the top IC layer where

$$\lambda_{freespace} = \frac{1}{\sqrt{\varepsilon_o \mu_o}\, f}$$

$$\lambda_{eff} = \frac{\lambda_{freespace}}{\sqrt{\varepsilon_r}}$$

$\lambda_{freespace}$ = Wavelength in free space (5mm for 60 GHz)

λ_{eff} = Effective wavelength (includes the effect of dielectric material)

ε_r = Relative constant of the dielectric material.

Today's conventional thinking hardly justifies on-chip antennas for low-power consumer devices due to high losses and low gains in the absence of compensating structures such as dielectric lenses. Indeed, typical on-chip antennas have only 10% efficiency and negative gain. However, if very high gain antenna structures can be designed and fabricated on chip in sub millimeter sizes, then the benefits of extreme cost reduction and improved design flexibility may outweigh the use of more efficient off-chip antennas that require more expensive and complex manufacturing processes [2-4].

Thus since the on chip antennas have very low gains, to compensate this effect the dielectric antennas are placed above and below the on chip antennas. This technique has the effect of reducing the energy lost in the substrate modes. A dielectric lens above the antenna reduces the difference in the dielectric constants above and below the antenna (without the lens above the antenna, the dielectric constant below the antenna is that of the silicon substrate, while that above is of air).This lens has the effect of increasing the antenna's radiation intensity away from the substrate and reducing energy lost into the substrate. The lens above the antenna should be constructed of a material with a dielectric constant equal to or larger than that of the substrate that supports the antenna (e.g., a dielectric lens of silicon dioxide ($\varepsilon_r = 4$) above an antenna on doped silicon ($\varepsilon_r = 4$) will not substantially improve performance.) [2-4]

Single on chip antennas are not adequate for achieving acceptable link setup at 60 GHz. Thus 60 GHZ require the use of antennas arrays on chip or in package to meet the link budget requirements. In [2-5], the advantage of using the antennas array for the 60 GHz technology has been illustrated. Arrays offer the best means of attaining a tight antenna beam pattern with the most flexibility for steering the antenna and in creating a system design. The disadvantages of using arrays are the increase in area and power required for many antenna elements, and the added implementation of beam-steering protocols, although higher frequency bands will make on chip arrays much smaller and thus easier to integrate. However instead of using the phased array antennas which require expensive and complex integration of lossy and bulky circuits, Shifted-beam antennas can use to as an alternative because they have fixed multiple beams that can be easily selected individually. In this thesis, the later has been implemented using the microstrip technology.

2.4 Antenna Arrays

A single antenna, patch, dipole, etc, has normally a wide radiation pattern (low directivity) and relative low gain. Also, it's very complicated or impossible to aim the main beam in a desired direction without physically moving the antenna. For this reason, antenna arrays are widely used.

"When two or more antennas equal to each other are used together, the combination is called "antenna array", "array antenna" or simply "array""

2.4.1 Concept of Antenna Arrays

An array consists of a group of identical antennas fed with particular amplitudes and phases in order to obtain the desired radiation pattern. With this technique it is not only possible to control the main beam direction, but also control the sidelobe characteristics. The gain and directivity are also enhanced in an array. The bigger the array is, the more directivity and gain the array has. Therefore arrays are very interesting for space communications, since extremely high gain and narrow beams (high directivity) are required.

Due to the discrete nature of array elements, the "amplitude and phase" of each element can be individually controlled. These amplitude and phase are so called excitation coefficients. These coefficients are usually represented by complex number in time harmonic regime. The total field of an array is determined by the vector addition of the fields radiated by the individual elements. The current in each element is determined by the separation of the elements. In [2-1], five controls are given through which desired shape of the overall patterns of an array can be controlled.

1. Geometric configuration of overall array.
2. Relative displacement between array elements.
3. Excitation amplitude of individual element.
4. Excitation phase of individual element.
5. Relative pattern of individual element.

2.4.2 N-Element Linear Array

In N element linear array, the antenna elements are placed in a straight line along an axis (x, y or z) as shown in Fig 2.2. The amplitude of each of the elements is assumed to be identical but each of the elements have progressive phase shift that depends on the distance between the elements i-e d. In the far field, the total E of the linear array is as follows:

$$E = E_o(I_o + I_1 e^{jkdcos\theta} + K + I_{N-1} e^{jk(N-1)dcos\theta})$$

$$E = E_o \sum_{n=0}^{N=1} I_n e^{jnkdcos\theta}$$

where E_o is the field radiated by basic antenna located at origin and is fed by 1A and $I_n = a_n e^{jn\alpha}$. I_n has progressive phase shift α and a_n are the source coefficients.

$$E = E_o \sum_{n=0}^{N=1} a_n e^{jn(kdcos\theta+\alpha)}$$

$$E = E_o \sum_{n=0}^{N=1} a_n e^{jn\psi}$$

and $\psi = kdcos\theta + \alpha$ is defined as the electrical angle where d is the distance between adjacent antennas, theta is the elevation angle, α is the progressive phase of the feed and k is the wave number given as $k = 2\pi/\lambda$.

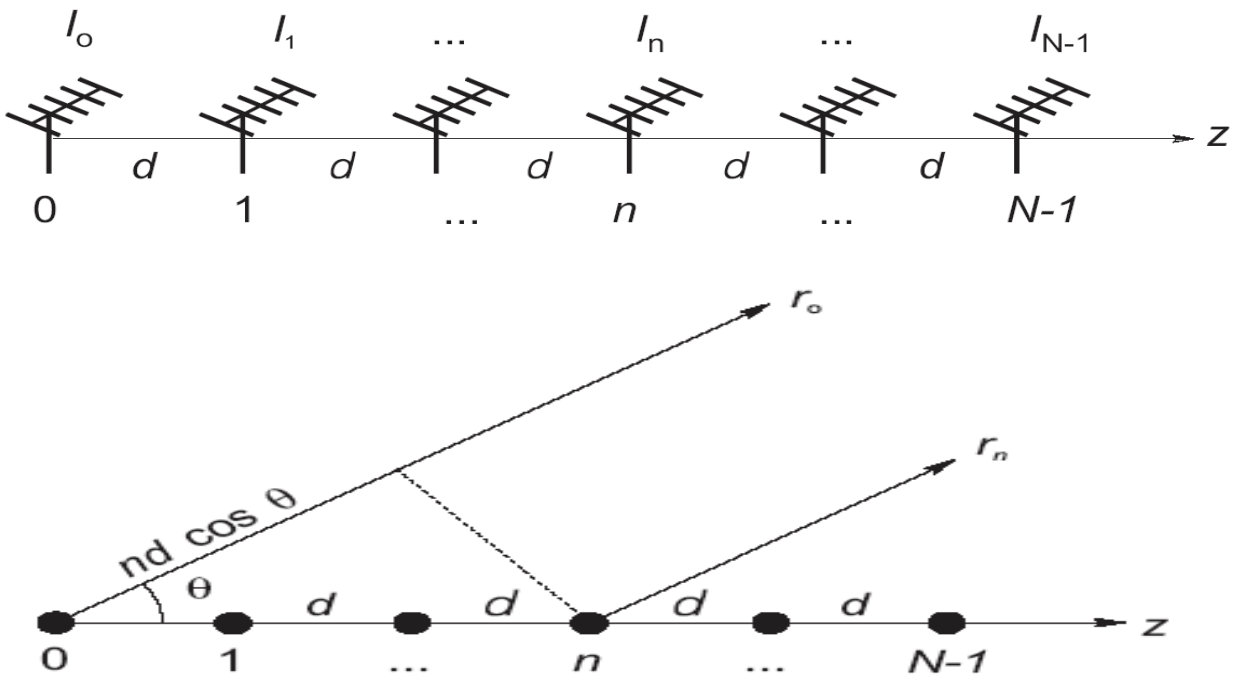

Fig 2.2: N Element Linear Array and its Far field interference

2.4.3 Array Factor

The array factor is the representation of the interference between the radiations of N elements of array. The array factor depends on the geometric configuration of the array i.e. number of antenna elements, shape of antenna elements, excitation of each element, and distance between the elements and frequency of operation. For this reason one array factor pattern can be obtained from different types of antenna resulting in different final radiation patterns. Thus the final pattern of the array is the multiplication of the array factor with the pattern of single element radiating individually as shown in Fig 2.3.

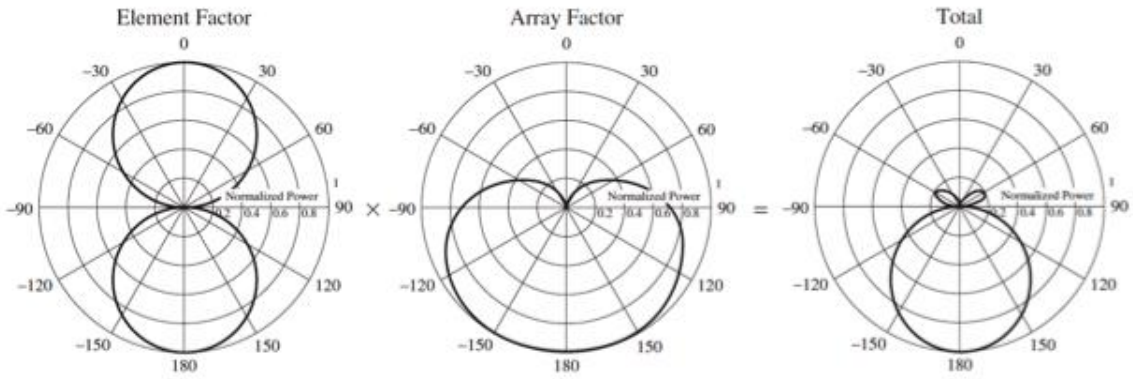

Fig: 2.3 Element Factor, Array factor and Total pattern (Array Multiplication) [2-1]

$$\boldsymbol{Total\ Pattern = Element\ Factor\ \times Array\ Factor = Eo * AF(\psi)}$$

Thus from the previous section we can conclude that the array factor is:

$$AF(\psi) = \sum_{n=0}^{N=1} a_n e^{jn\psi}$$

which is the function of the electrical angle ψ. Following are the few array factor properties:

- It is a periodic function in ψ with 2π period.
- It is the Fourier Transform (FT) of the coefficient sequence a_n
- If the source coefficients a_n are positive real numbers the maximum is at $\psi = 0$.
- Since the θ angle is between 0 and 2π, only the AF interval $\psi \epsilon [-kd + \alpha, kd + \alpha]$ belongs to the radiation pattern. It is called the "Visible region" as shown in Fig 2.4.
- Since AF is periodic with 2π period, there are periodic maxima .If those maxima are located inside the visible region, then multiple maxima of radiation appear in the real space pattern. These periodic maxima are called *grating lobes*.

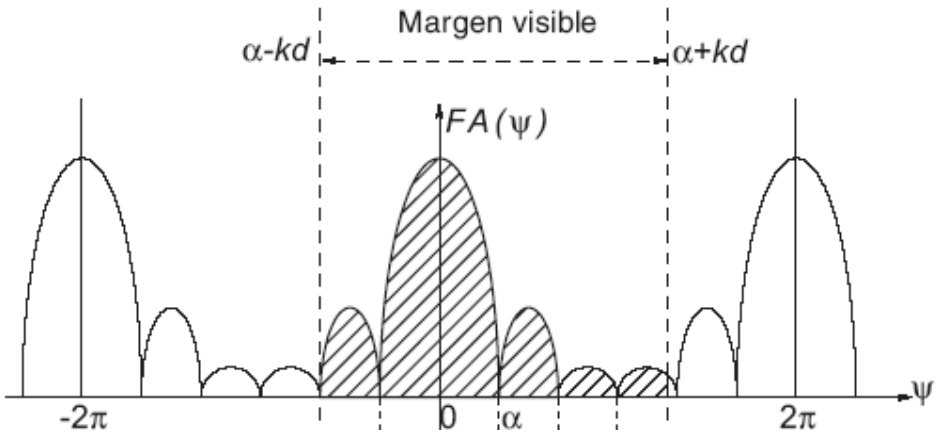

Fig 2.4: AF(ψ) has a symmetry of revolution around z-axis

2.4.4 Broadside Linear Array

Broadside array has the maximum radiation normal to the axis of array. To optimize the design, the maxima of the single element and of the array factor must be at $\theta = 90°$. Thus the single element can be selected which has normal maximal radiation to its surface and then array can be formed by proper separation and excitation of individual radiators. The maximum of the array factor occurs when

$$\psi = kdcos\theta + \alpha = 0$$

and since the maximum direction in case of broadside array is at $\theta = 90°$, thus

$$\alpha = 0$$

Thus for a broadside radiation, each element of the array must have same phase along with same amplitude. The separation between elements can be of any value but to avoid the grating lobes it should not be a multiple of the wavelength ($d \neq n\lambda, n = 1, 2, 3 \ldots$). If $\alpha = 0$ and $d = n\lambda, n = 1, 2, 3 \ldots$ then

$$\psi = 2\pi nCos\theta$$

$$\psi = \pm 2\pi n \; at \; \theta = 0°, 180°$$

This value gives its array factor maximum value and thus additional maxima are obtained at $\theta = 0°, 180°$. In this thesis, since the broadside array is required without the grating lobes so the required $\alpha = 0$ and the separation between the elements must me less than the wavelength [2-1]

2.4.5 Feeding Network

To ensure proper amplitude and phase excitation of all the elements of the array, the feeding network of the array holds good importance. There are many arrangements for distributing the input power from the source to the linear array. Most common of these networks are: [2-7]

Series Feed

This network arrangement is the simplest one and is shown in Fig 2.5. The radiating elements are placed in series and are connected by intervening the transmission line. The required spacing between the elements for proper excitation determines the length of transmission lines between the radiating elements. Each element also has two transmission lines expect the last one.

The input power is fed at one of the ends. A fraction of the input power is radiated by the each element and the rest is transmitted to the next element. When the frequency changes, the progressive phase shift along a series-fed changes because the electrical length of the transmission line between the radiating elements. This causes the main beam to change its direction and enables the frequency scanning. Thus for this reason in this thesis the series fed array are being analyzed.

Series Compensated feed (out of line feed)

This type of arrangement is same as series as shown in Fig 2.6 but the radiating elements are out of the transmission line and each radiating element has only one transmission line. The lengths of the paths between the elements can be adjusted to make the array frequency insensitive so that the beam

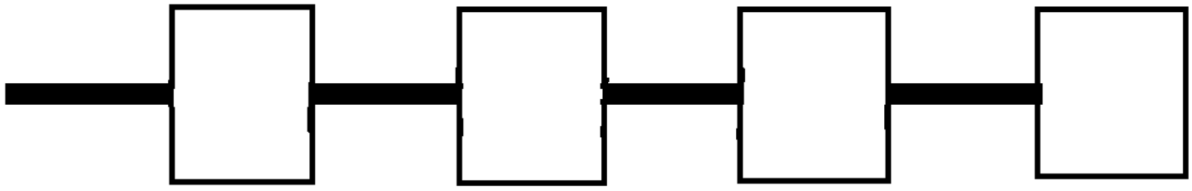

Fig 2.5: Series-Fed Linear Array

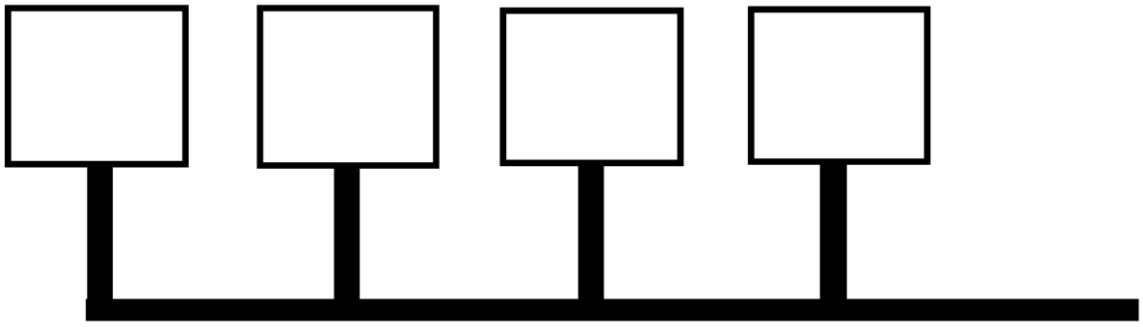

Fig 2.6: Out of Line Series-Fed Linear Array

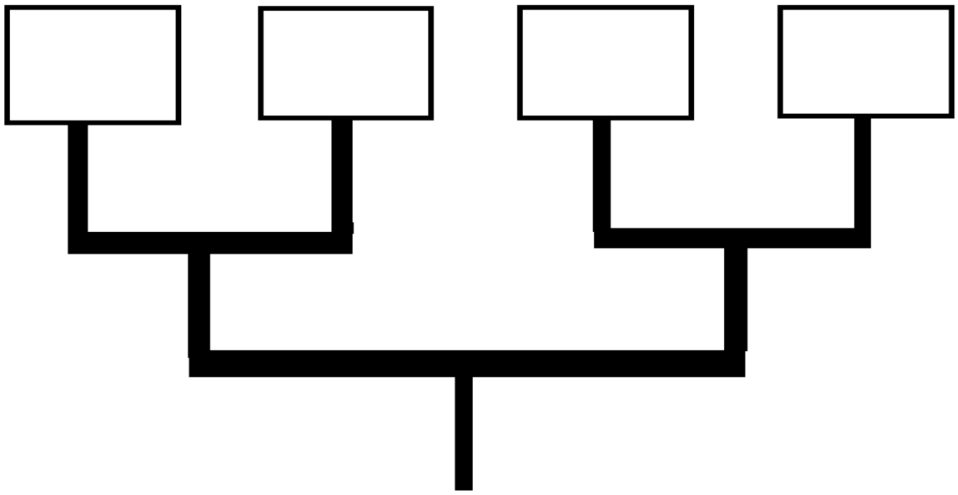

Fig 2.7: Parallel-Fed Linear array

direction does not change with the shift in frequency. However additional transmission line adds more losses to the structure. In [2-8], meandered transmission lines have been used to make the array frequency insensitive.

Corporate (or parallel) Feed

As shown in Fig 2.7, the power is distributed into all of the radiating elements by using the power splitter. The path length to each of the element is same so each array element has same phase and amplitude. Thus huge space is required to implement a large array. To get required amplitude at each of the array element, only the impedance of the transmission line can be changed in the feeding network. Due to the complex power-dividing network there are more losses.

Comparison between Series and Parallel Feeds

Table 2.1 shows the summary of advantages and disadvantages of series-fed and parallel-fed arrays.

Series-Fed Array	Parallel-Fed Array
Frequency dependent beam direction	Frequency independent beam direction
Bandwidth is narrow	Bandwidth is wide
Efficient in space usage	Poor in space usage
Less losses due to transmission lines	More loss due to complex power dividing network

Table 2.1: Comparison between Series-fed and Parallel-fed Array (the table has been modified from [2-7])

References

2-1 “Antenna theory, Analysis and Design”, CA Balanis, 2nd ed, Wiley., 1998

2-2 IEEE Standards Board, “IEEE Standard Definitions of Terms for Antennas”, IEEE Std 145-1993, Mayo 1993.

2-3 “On-Chip Integrated Antenna Structures in CMOS for 60 GHz WPAN Systems” Felix Gutierrez, Jr. *Student Member*, *IEEE*, Shatam Agarwal, *Student Member*, *IEEE*, Kristen Parrish, *Student Member*, *IEEE*, and Theodore S. Rappaport, *Fellow*, *IEEE*, IEEE JOURNAL ON SELECTED AREAS IN COMMUNICATIONS, VOL. 27, NO. 8, OCTOBER 2009

2-4 "State of the Art in 60-GHz Integrated Circuits and Systems for Wireless Communications," T.S. Rappaport, J.N. Murdock, and F. Gutierrez, Proceedings of the IEEE, vol.99, no.8, pp.1390-1436, Aug. 2011

2-5 “A 16-element phased-array receiver IC for 60-GHz communications in SiGe BiCMOS” S. K. Reynolds, A.S. Natarajan, T. Ming-Da, S. Nicolson, C. Z. Jing-Hong, L. Duixian, D. G. Kam, O. Huang, A. Valdes-Garcia, and B. A. Floyd, Proc. IEEE Radio Freq. Integr. Circuits Symp., May 23–25, 2010, pp. 461–464, DOI: 10.1109/RFIC.2010. 5477306

2-6 “Microstrip Antennas: The Analysis and Design of Microstrip antennas and Arrays”, D. Pozar and D. Schaubert, Wiley IEE express, 1995

2-7 “Design of a Low Side Lobe Short Series-Fed Linear Array of Microstrip Patches” A. Benalla and K. C. Gupta, Electromagnetic Laboratory Scientific Report No. 93, October 1987, University of Colorado

2-8 “Modern Antenna Handbook”, CA Balanis, ISBN: 978-0-470-03634-1, Wiley, Sept 2008.

3. Microstrip Patch Antenna and Coplanar Waveguide

3.1 Patch Antenna Analysis

The Patch antenna design is considered in this thesis because of its directivity, low profile and ease of fabrication. The importance of microstrip radiators was realized when researchers noted that almost half of the power in a microstrip radiator escapes as radiation. Thus, a microstrip radiating patch with considerable radiation loss was defined as microstrip antennas. Later, it was proved that this radiation mechanism was arising from the discontinuities at each end of the microstrip transmission line [3-1].

The basic form of a patch antenna consist of a flat plate over a dielectric substrate that at the same time is over a ground plane. The metal patch is normally made from copper foil but the substrate material can vary between different types, depending on which ε_r it's needed. Those three layers are the minimum elements to define a patch antenna.

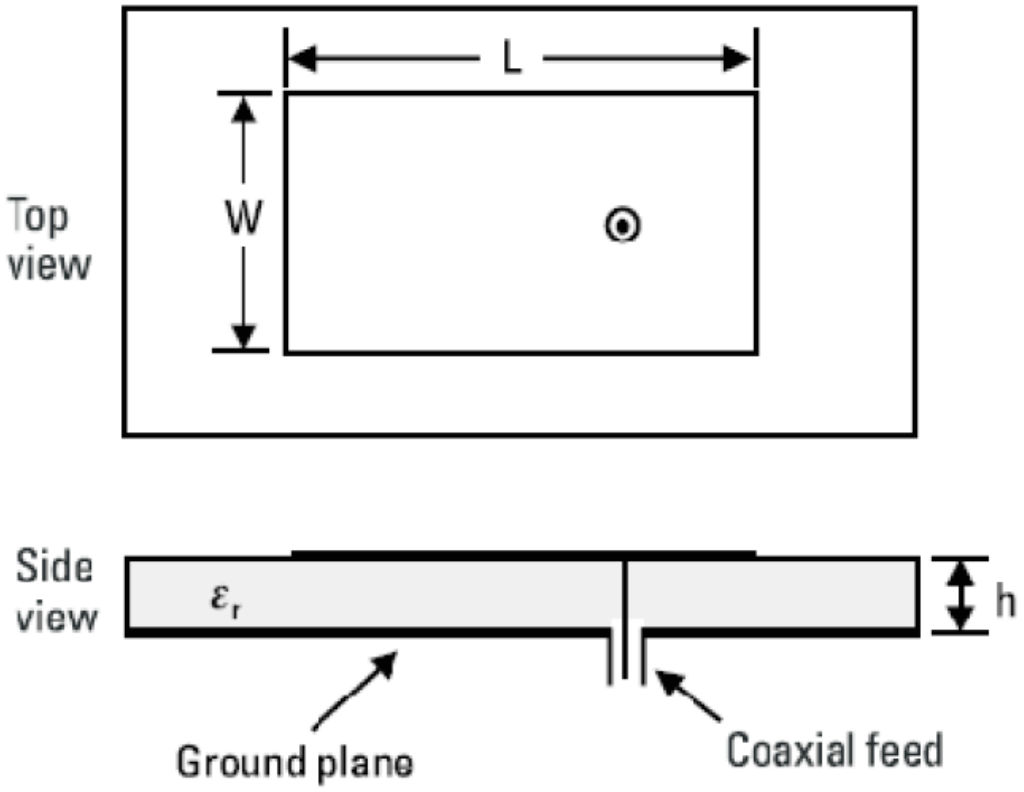

Fig 3.1: Top and Side view of Rectangular Patch antenna

The radiating patch can be designed with a variety of shapes such as: square, circular, triangular, semicircular, sectorial, and annular ring shapes; but rectangular and circular configurations are the most commonly used configuration because of ease of analysis and fabrication.

When the patch is excited by a feed line, charge is distributed on the underside of the patch and the ground plane. At a particular instant of time the attractive forces between the underside of the patch and the ground plane tend to hold a large amount of charge. And also the repulsive forces push the charges to the edge of the patch, creating a large density of charge at the edges. These are the sources of fringing field as shown in fig 3.2. Radiation from the microstrip antenna can occur from the fringing fields between the periphery of the patch and the ground plane.

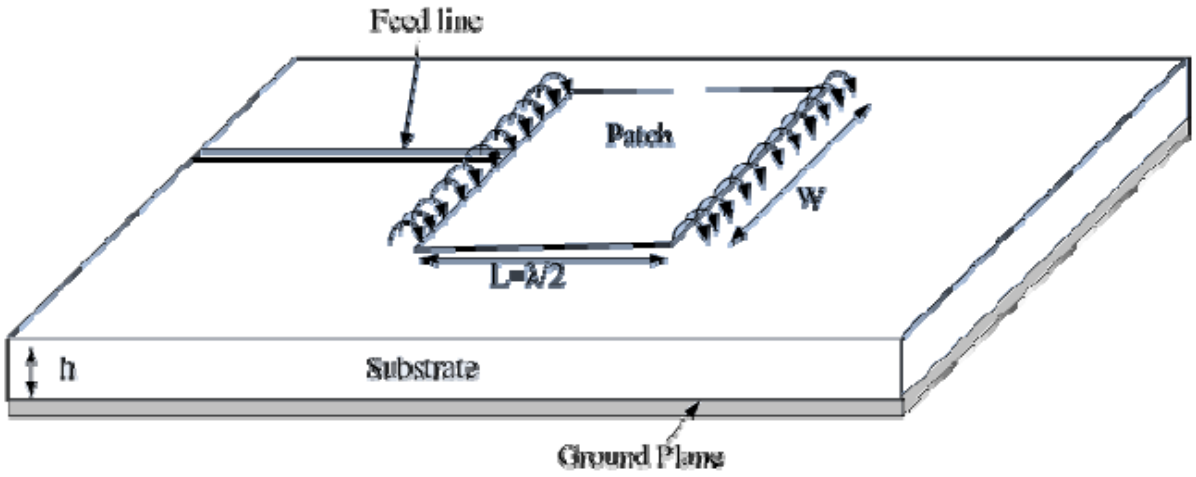

Fig 3.2: Fringing Fields

3.1.1 Methods of Analysis

There are several methods of analysis for analyzing the patch antenna and most of them consider the 2D planar element. The three most common methods of analysis are transmission line model, cavity model and full wave model. The transmission line model is the simplest mode, gives a good physical insight but it is not very accurate. The cavity model gives good accuracy and physical insight, but it is more complex. And finally, the full wave model is by far the most accurate and versatile model, offers more options, but it give less physical insight and is much more complex to use than the other two models.

Transmission Line Model

Transmission line Model consider rectangular patch antenna to be parallel plate transmission line connecting to radiating slots each of width W and height h as shown by fig 3.2. Transmission line is not accurate and lacks versatility but it is the easiest one and gives physical insight and field distribution of the antenna.

As explained earlier, patch antenna has a length L, width W and thickness h (substrate). To obtain TM10 mode, the length of the patch should be less than $\lambda/2$. Thus as given in chapter 2, the wavelength is calculated considering the dielectric constant ε_r, and the length of patch is thus

$$L = \frac{\lambda_{eff}}{2} = \frac{\lambda_{freespace}}{\sqrt{\varepsilon_r}}$$

The Voltage, Current and impedance distributions are shown in fig 3.3. The voltage has maximum and minimum values at the edge on each side of length and zero value in the middle due to the fact that the

edges appear as open circuits. By contrast, the current intensity has zero value at edges and maximum value in the middle. Thus it can be seen that there is no field variation along width W. Since the fields are in contra-phase at edges it causes the normal components of the field to cancel each other in the broadside direction. However, the tangential components are in phase and cause radiation normal to the patch surface.

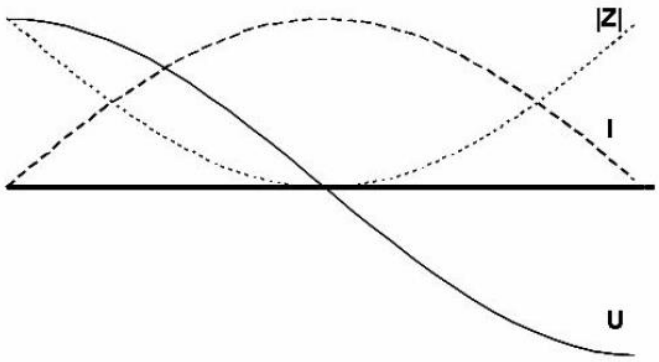

Fig 3.3: V, I and [Z] distribution

The slots of the patch give very high impedance terminations at the end of the transmission line, thus the structure is expected to be highly resonant which is dependent on the length of the patch. The resonant length of the patch antenna is therefore not equal to physical length but is slightly more than the length L due to the fringing effects as shown in fig 3.4. The effective Length L_{eff} is

$$L_{eff} = L + \Delta L$$

From [3.7],

$$\Delta L = 0.412 \left[\frac{(\varepsilon + 0.3)(\frac{W}{h} + 0.264)}{(\varepsilon - 0.258)(\frac{W}{h} + 0.8)} \right] h$$

There is no radiation along the length L of the patch, so they are called non-radiating edges. Since the width W of the patch is responsible for radiation thus the value of the width can help antenna to radiate more efficiently. It value is

$$W = \frac{c}{2f\sqrt{\frac{\varepsilon_r + 1}{2}}}$$

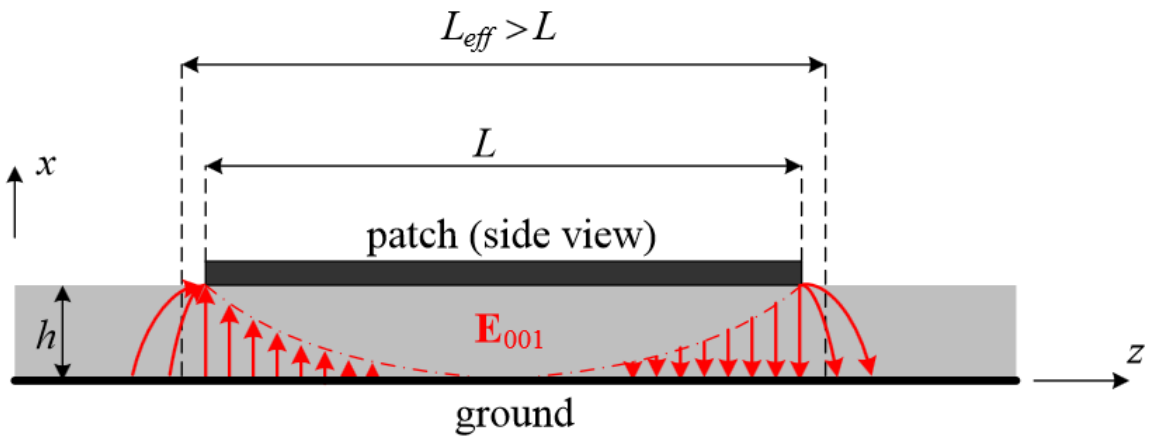

Fig 3.4: L_{eff} of the patch is greater than the length L of the patch due to fringing fields

3.1.2 Advantages and Disadvantages

The microstrip antenna has proved to be an excellent radiator for many applications because of its several advantages, but it also has some disadvantages; however some of them can be overcome using new techniques of feeding, configuration of the patch, etc.

Advantages

- They are light in weight and take up little volume because their low profile. They can be made conformal to the host surface.
- Low fabrication cost, hence can be manufactured in large quantities.
- They are easier to integrate with other microstrip circuits on the same substrate.
- They support both, linear as well as circular polarization.
- They can be made compact for use in personal mobile communication and hand held devices.
- They allow multiple-frequency operation, because you can use stacked patches.
- Mechanically robust when mounted on rigid surfaces.

Disadvantages

- Narrow bandwidth.
- Lower power gain.
- Lower power handling capability.
- Polarization impurity.
- Surface wave excitation.
- Extraneous radiation from feeds and junctions.
- Poor end fire radiator except tapered slot antennas.

3.1.3 Feeding Techniques of Microstrip antennas

The feeding method or excitation technique is an important design parameter because it influences to the input impedance, the polarization characteristic and the antenna efficiency. As the feeding method influences to the input impedance, is often used for purposes of impedance matching.

Microstrip antennas can be excited or fed directly or indirectly. A microstrip antenna is fed directly using a connecting element such as the use of a coaxial probe or by a microstrip line, when it is excited indirectly, there is no direct metallic contact between the feed line and radiating patch, and it could be using proximity coupling or by aperture coupling [3-2].

Coaxial or Probe Feed

In case of feeding the patch antenna with coaxial or probe feed, the center conductor coaxial connector extends through the substrate and then is soldered to the radiating patch, while the outer conductor is connected to the ground plane as shown in fig 3.1.

Advantage: The feed can be placed at any point on the patch, which allows to achieve the perfect matching with the input impedance of the patch.

Disadvantage: Geometry does not remain completely planar because a hole has to be drilled in to the substrate so that the inner conductor of the coaxial can be soldered to the patch. Also the configuration becomes asymmetrical because of this feeding option.

Microstrip Line Feed

The microstrip patch is fed with a microstrip line as shown in fig 3.5 (a) where the strip line connects the patch at the edge. So the impedance of the line should be matched to the edge impedance of the patch. There are several techniques to achieve the impedance patching which are inset feed, non-radiating edge feed and use of quarter wave transformers as shown if fig 3.5 (b) (c) and (d) respectively.

Advantage: This feed provides a planar structure so they are easy to fabricate.

Disadvantage: There are radiations from the feed especially in case of millimeter-wave range where the width of the feed line becomes comparable to the size of the patch.

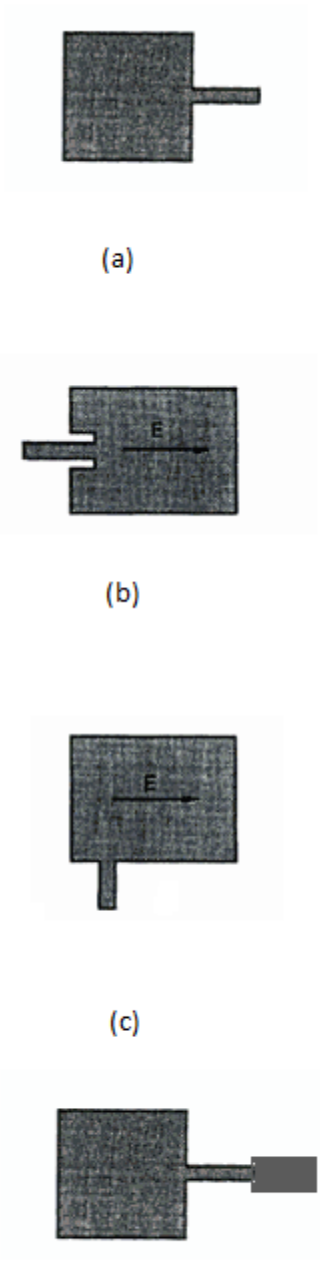

Fig 3.5: (a) Microstrip line feed (b) Inset Feed (c) Microstrip line feed at non-radiating edge (d) Microstrip line feed with quarter wave transformer [3-1]

Proximity and Aperture Coupling

There are other methods for indirect feeding of the patch such as proximity coupling and aperture coupling. These types of feedings are basically used for increasing the bandwidth of the patch. In proximity coupling there is electromagnetic coupling between the feed line and the patch while both the antenna and the feed line are on the same plane. This feed provides the largest bandwidth as compared with other couplings with the advantage of no increase in thickness of the antenna [3-2]. In aperture coupling, the ground plane separates the radiating patch and the microstrip feed line. The coupling between the radiation patch and the feed line is made through an opening slot or an aperture in the ground plane. There are two advantages for this technique, one is that it isolates the radiating patch from the feed and shield it with the ground plane and second is that the choice of different substrate can result in better antenna performance [3-1]. However this technique comes with the drawback of layered structure and huge thickness. Fig 3.6 shows these two techniques.

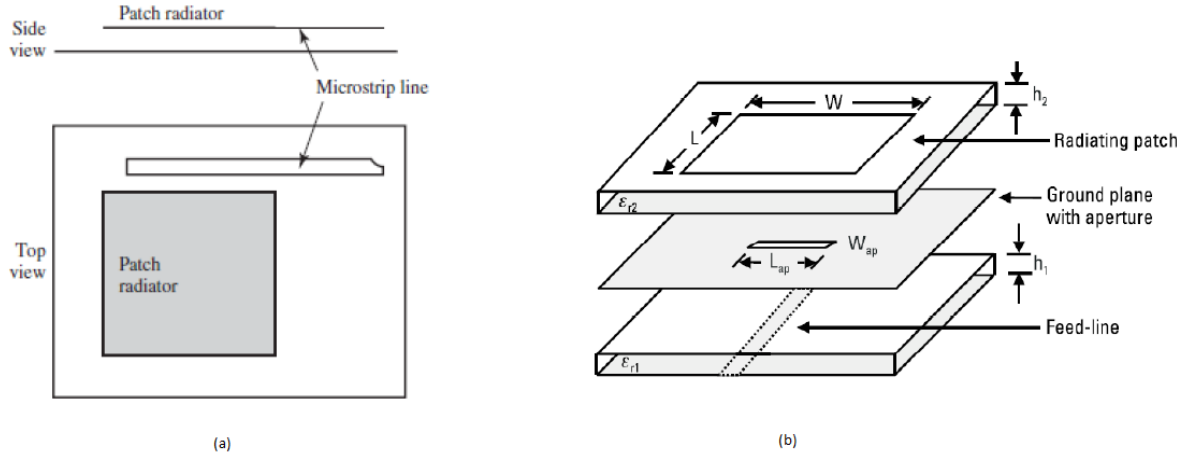

Fig 3.6: Indirect feed (a) Proximity Coupling (b) Aperture Coupling [3-1]

3.2 Coplanar waveguide Feed

Microstrip antennas have found many applications in millimeter wave technology. In especially MMIC´s the coplanar waveguide feeding technique has gained very huge popularity to due there low attenuation and dispersion while making fabrication of such circuits very easy. [3-3], [3-4]. For this purpose and also due the availability of G-S-G probe system in the Antenna Lab of UPC, in this thesis the CPW feed line is being used as the transmission line for the excitation of our 60 GHz patch antenna. Thus the basic concept of the coplanar waveguide are discussed in the next section in detail.

3.2.1 Coplanar Waveguide

Coplanar waveguide is an alternative to microstrip line. The CPW has been invented by Cheng P. Wen in 1969 while he was working in Sarnoff Laboratories [3-5]. “A Coplanar waveguide consists of a strip of thin metallic film on the surface of a dielectric slab with two ground electrodes running adjacent and parallel to the strip” [3-6]. A CPW layout is shown in fig 3.7.

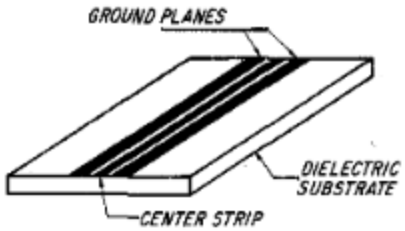

Fig 3.7: CPW, a surface strip transmission line [3-6]

Following are the few features of CPW [3-5]:

- The dimensions of the center strip, the gap, the thickness and permittivity of the dielectric substrate determined the effective dielectric constant, characteristic impedance and the attenuation of the line.
- The gap in the coplanar waveguide is usually very small and supports electric fields primarily concentrated in the dielectric. With little fringing field in the air space, the coplanar waveguide exhibits low dispersion. In order to concentrate the fields in the substrate area and to minimize radiation, the dielectric substrate thickness is usually set equal to about twice the gap width.
- CPW has a zero cut-off frequency (suitable for wideband), but its low order propagation mode is indicated with Quasi-TEM because it is not a real TEM mode. At higher frequencies, the field becomes less-TEM, and more TE in nature. The CPW magnetic field is elliptically polarized. The E and H field distribution in CPW is shown in fig 3.8.
- CPW it is a printed circuit analogs of the three-wire transmission lines.

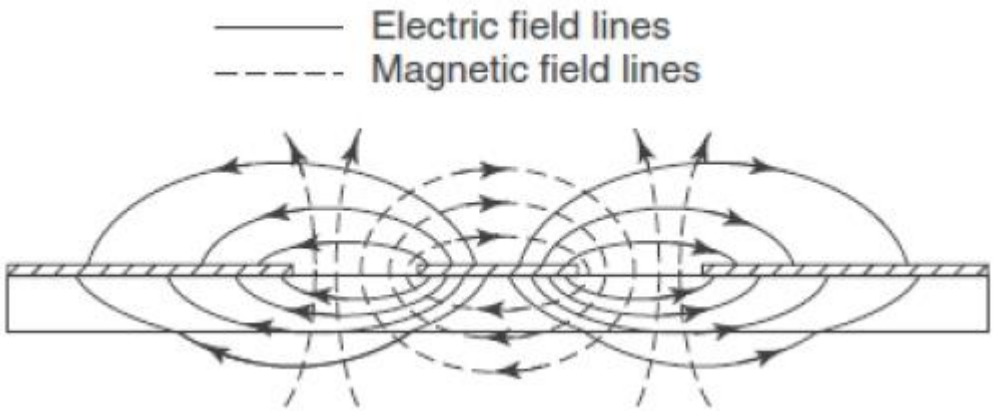

Fig 3.8: Electric-E and Magnetic-H felid distribution across CPW

- CPW has two ground planes, which must be maintained at the same potential to prevent unwanted modes from propagating. If the grounds are at different potentials, the CPW mode will become uneven, with a higher field in one gap than the other.
- In the CPW, the effective dielectric constant is approximately independent of geometry, and simply equal to the average of dielectric constants of air and the dielectric substrate.
- Frequency dispersion for CPW is generally small, but there is a mild dependence on line dimensions, and narrow lines are less frequency dispersive than wide lines.

- **Grounded Coplanar Waveguide** (GCPW) is used on printed circuit boards as an alternative to Microstrip line as shown in fig 3.9. The gap *s* between the strip and ground is usually more than the thickness *h* of the substrate, so the GCPW field is concentrated between the strip and the substrate ground plane, and GCPW behaves like Microstrip.

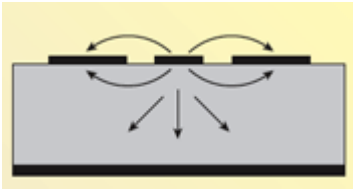

Fig 3.9: Grounded Coplanar Waveguide

- In addition, to avoid field radiation in the air, it is very important to use substrates with a high dielectric constant, with recommended values greater than 10, so that the electromagnetic field is mainly concentrated inside the dielectric.
- In CPW a ground plane exists between any two adjacent lines, hence cross talk effects between adjacent lines are very week. As a result, CPW circuits can be made denser than conventional Microstrip circuits.

3.2.2 Advantages and Disadvantages of CPW

A list of the advantages and disadvantages of CPW are being presented in the following sections

Advantages

- CPW gives huge circuit isolation because of the RF grounds in the traces. Many High-resolution RF switches use grounded CPW to get 60 dB of isolation.
- Bottom reference plane of the grounded CPW provides structural strength.
- CPW gives lower conductor losses and dispersion.
- Since there are no connecting via, so CPW has low radiation losses at the discontinuities.
- Lower crosstalk improves MMIC layout density from 30% to 50% compared to microstrip.
- CPW provides 30% cost reduction in MMIC´s fabrication because of simpler processing steps and elimination of backside processing.
- Also the impedance of the CPW transmission lines are lower than the usual microstrip lines which allows the ease in the impedance matching of the circuit.

Disadvantages

- CPW side strips generate both odd and even modes current that can cause serious mode coupling.
- PW without conducting plane has lower thermal dissipation and lower structural strength.
- High frequency losses due to over modes are more prevailing on CPW than microstrip.
- In general, CPW experience higher losses compared to microstrip.

References

3-1 D. M. Pozar and D. H. Schaubert, “Microstrip Antennas: The analysis and design of microstrip antennas and arrays”, IEEE Press, New York, 1995.

3-2 G. Kumar, K. P. Ray: “Broadband microstrip antennas”. Artech House, 2003.

3-3 W. Menzel, W. Grabherr “A Microstrip Patch Antenna with Coplanar Feed Line”. IEEE Microwave and Guided Wave Letters, vol.1, no.11, page 340 –342, November 1991.

3-4 K. Hettak, G. Delisle, “A Novel CPW Coupled Patch Antenna Topology for Dual Band Op e-ration” Antenna and Propagation Symposium, IEEE, page 1048 –1051, 2004

3-5 Microstrip, Stripline, and CPW Design *Iulian Rosu, YO3DAC / VA3IUL*

3-6 Cheng P. Wen, IEEE Member, "Coplanar Waveguide: a surface strip transmission line suitable for nonreciprocal gyromagnetic device applications", IEEE Transactions on Microwave Theory And Techniques, VOL. MTT-17, NO.12, December 1969

3-7 The Microstrip Antenna Analysis and Design Using The TTL Method, Anthony R. N. Farias and Humberto C. Chaves Fernandes Department of Electrical Engineering - Technological Center Federal University of Rio Grande do Norte P.O.Box 1583, Tel/Fax: +55 84 215.3731, 59.072-970 - Natal - RN – Brazil, Journal of Microwaves and Optoelectronics, Vol. 1, No. 2, April 1998.

4. CPW fed Microstrip Patch Antenna Design and Results

4.1 Introduction

The project was started with the design of a single patch that is being fed by CPW feed line. The reason of choosing CPW as a feed line has been explained in chapter 3. The requirements of the antenna were the high bandwidth and small dimensions of the antenna. For obtaining an appropriate bandwidth the microstrip patch antenna was designed on two different substrates and each of the designs with their simulation and measurement results have been discussed in this chapter.

4.2 Design Specifications

The design of the patch antenna is shown in fig 4.1. All the tags, their identification and their values are given in Table 4.1 along with other design specifications. The length and width of the patch are obtained from the equations explained in chapter 3. Since the aim of the project is to get the antenna resonate at 60GHz which gives $\lambda = 5\ mm$, so the length of the antenna is L =$\frac{\lambda}{2} = 2.5\ mm$.

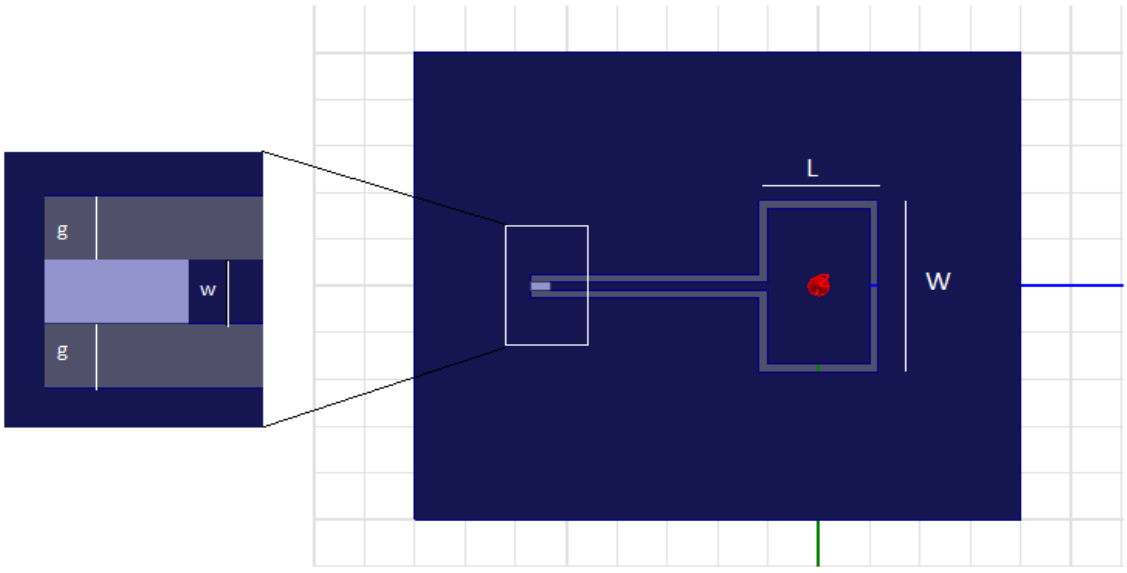

Fig 4.1: Design of CPW fed Patch antenna.

The reason of selection these dimension for CPW feed line width and gap is because the GSG probe system for feeding the antenna that is present at the Antenna lab of TSC department of UPC has 150 um pitch. Thus the CPW feed line width and gap has been selected to be 80 um, so that the CPW line can be fed with this GSG probe.

For the purpose of all the designs, configurations and simulations, the software used in this project is HFSS (High frequency Structural Simulator). All the simulation results shown in the rest of the thesis are

obtained from this software which will be later compared with measured results. A brief description of the software can be found in Appendix A.

Required Design Specifications		
L	Length of patch	$L = \frac{\lambda_{eff}}{2} = \frac{\lambda_{freespace}}{\sqrt{\varepsilon_r}}$
W	Width of Patch	$W = \frac{c}{2f\sqrt{\frac{\varepsilon_r + 1}{2}}}$
g	Gap of CPW	80 um
w	Width of CPW Feed	80 um
BW	Required Bandwidth	57 GHz – 64GHz
fr	Resonant Frequency	60 GHz

Table 4.1: Required design Specifications for the single patch antenna

The antenna is required to resonate at 60 GHz and it is desired that the antenna is able to radiate over a long range of frequencies that is 57GHz-64GHz which is the frequency application band for WPAN systems. To obtain this large bandwidth, in this project two different substrates have been chosen for the design since the bandwidth of the small antenna depends on the dielectric constant of the substrate. Each of these designs have been presented and explained in the rest of the chapter.

4.3 Design of Single Patch antenna

Two different designs of patch antenna have been designed for obtaining larger bandwidth.

4.3.1 Design I

In the first design, Rogers R04350 with the dielectric constant of 3.66 has been used. The height of the substrate used is 10 MIL i.e. 0.254 mm. Since the length and width of the patch depends on the substrates dielectric value, thus the length of the patch is 0.26 λ and width of the patch is 0.32 λ. The width and gap of the CPW feed line are same as stated in the previous section. However the feed line length has been adjusted by performing multiple simulations to achieve the best impedance matching. The design parameters of the antenna are listed in table 4.2.

Rogers RO4350	
Permittivity (ε_r)	3.66
Loss Tangent (LossD)	0.004
Substrate Thickness (h)	0.254 mm
Patch Dimensions	
Length (L)	1.02 mm
Width (W)	1.67 mm
CPW Dimensions	
CPW feed Length	7.5 mm

Table 4.2: Design Parameter for Roger RO4350 substrate

As can be seen that the length and width of the patch antenna are not exactly 0.26 λ and 0.32 λ because modification have been performed in multiple simulation to achieve the best performance of the patch and return loss and resonant frequency at 60 GHz.

Simulation Results

With the said design parameters, the simulation results from HFSS are shown in fig 4.2, 4.3, 4.4 and 4.5. The return loss shows that the simulated bandwidth of antenna is from 58 GHz to 61 GHz (3 GHz) and the antenna is resonating at 59.6 GHz. The radiation pattern shoes the maximum gain obtained is approximately 2 dB at the broadside direction.

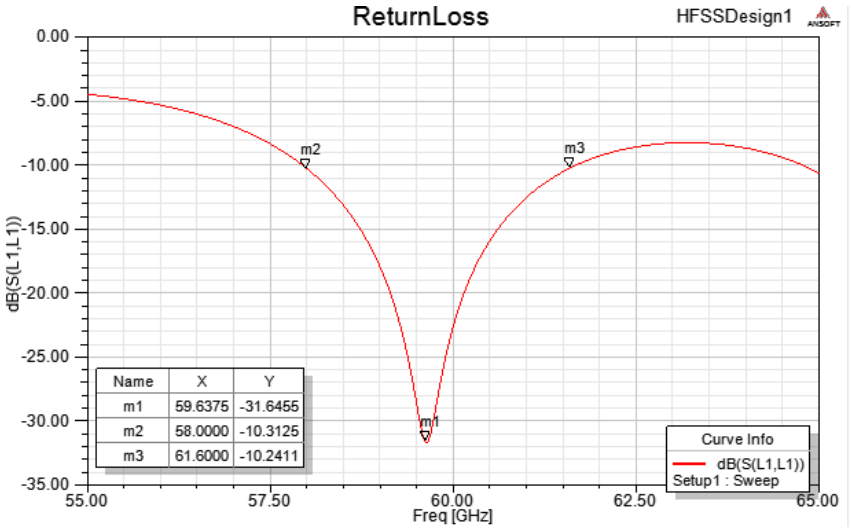

Fig 4.2: Simulated return loss for antenna design I (BW = 3GHz)

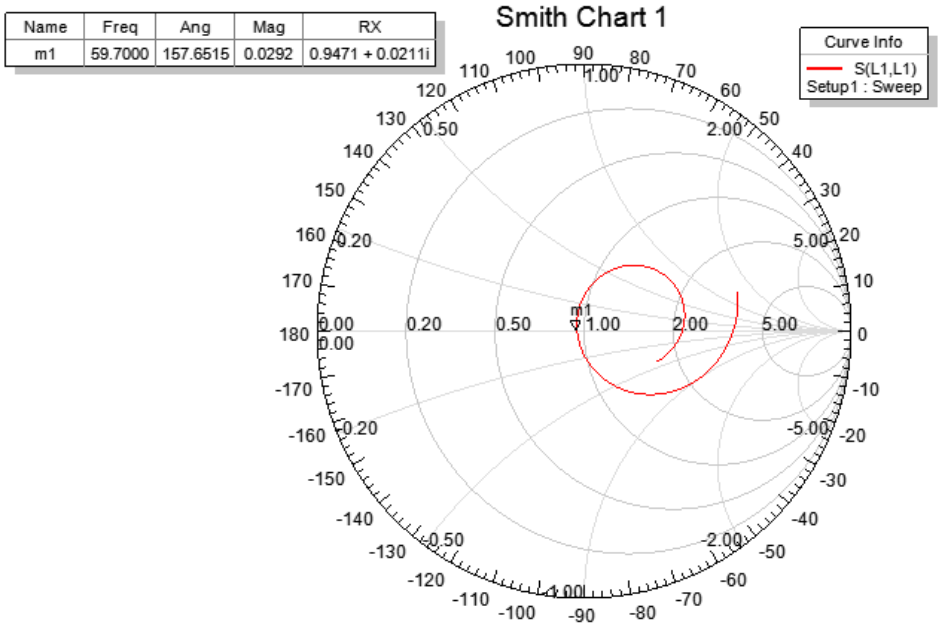

Fig 4.3: Simulated Smith Chart plot for this antenna design I

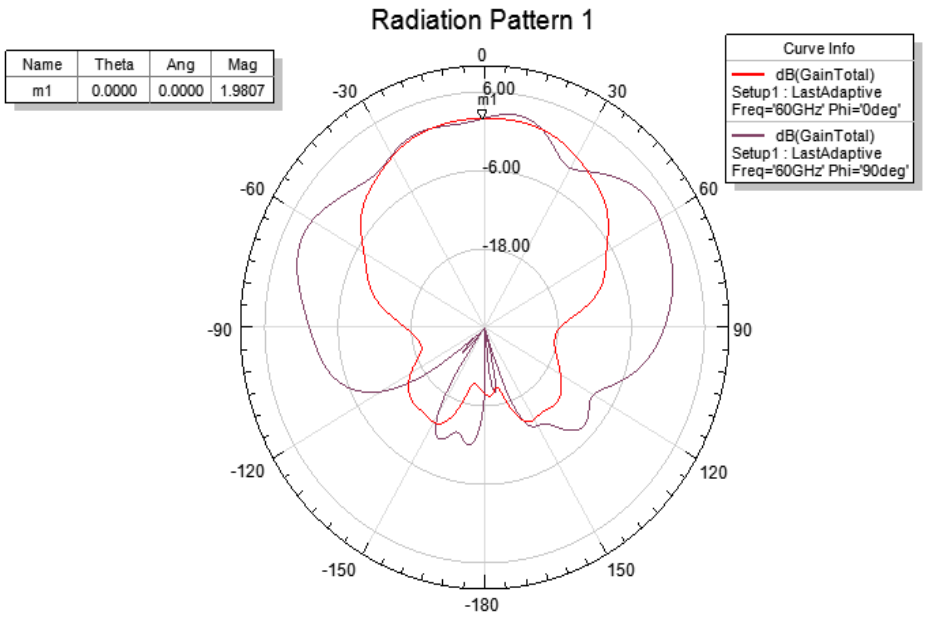

Fig 4.4: Simulated Radiation pattern for antenna design I (Gain = 2dB at 60 GHz)

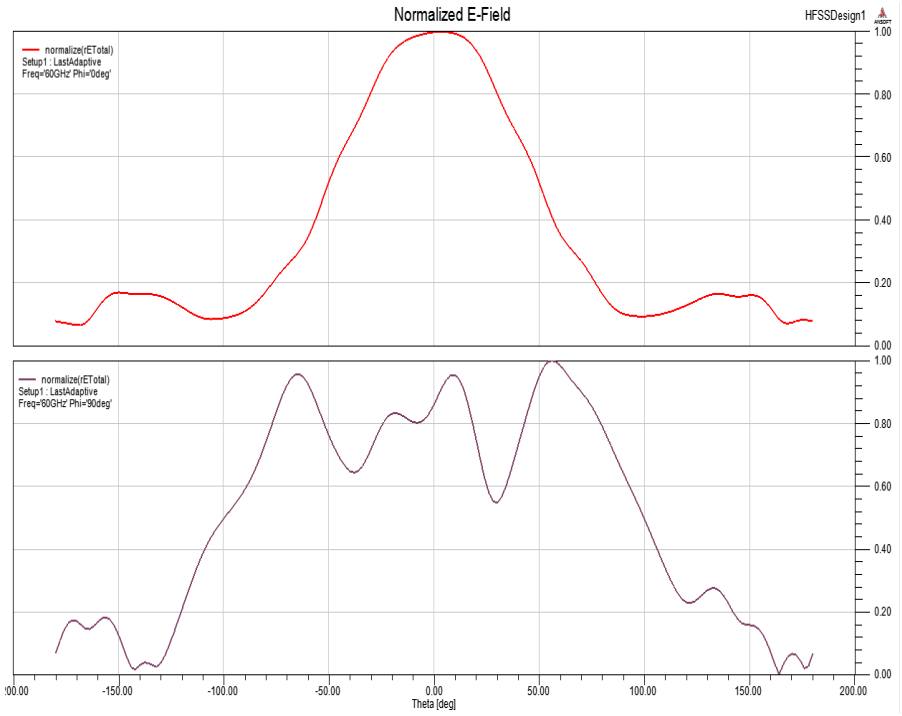

Fig 4.5: Simulated Normalized E for antenna design I

4.3.2 Design II

In order to increase the bandwidth it has been proposed to use dielectric substrate with the lower permittivity value. So in this design, Rogers RT/duroid 5880 with the dielectric constant of 2.2 has been used. The height of the substrate used is 15 MIL i.e. 0.381 mm. Since the length and width of the patch

depends on the substrates dielectric value, thus the length of the patch is 0.33 λ and width of the patch is 0.39 λ. The width and gap of the CPW feed line are same as stated in the previous section. However the feed line length is again adjusted by performing multiple simulations to achieve the best impedance matching. The design parameters of the antenna are listed in table 4.3.

Rogers RT/Duroid 5880	
Permittivity (ε_r)	2.2
Loss Tangent (LossD)	0.0009
Substrate Thickness (h)	0.381 mm
Patch Dimensions	
Length (L)	1.3 mm
Width (W)	1.8 mm
CPW Dimensions	
CPW feed Length	2.1 mm

Table 4.3: Design Parameter for Roger RO4350 substrate

As can be seen that the length and width of the patch are modified in multiple simulation to achieve the best performance of the patch and return loss and resonant frequency at 60 GHz. Another important change made in this design from the previous design is that the height of the substrate is also increase from 10 MIL to 15 MIL. The motivation is to increase the bandwidth as the BW of the antenna increases by increasing the height of the substrate. However the drawback is the accumulation of the fields inside the substrate also increases.

Simulation Results

With the said design parameters, the simulation results from HFSS are shown in fig 4.6, 4.7, 4.8 and 4.9. The return loss shows that the simulated bandwidth of antenna is from 57 GHz to 62 GHz (5 GHz) and the antenna is resonating at 60 GHz. The radiation pattern shoes the maximum gain obtained is approximately 2 dB at the broadside direction.

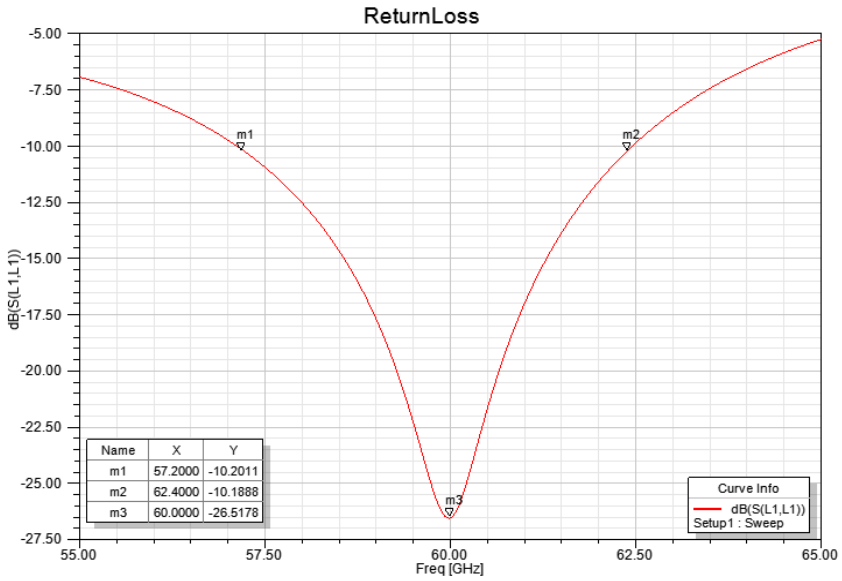

Fig 4.6: Simulated return loss for antenna design II (BW = 5GHz)

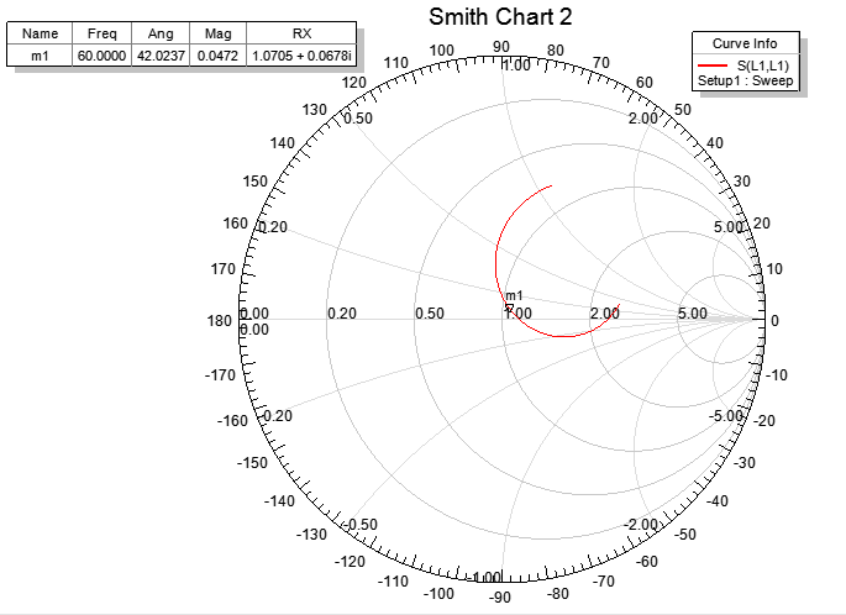

Fig 4.7: Simulated Smith Chart plot for this antenna design II

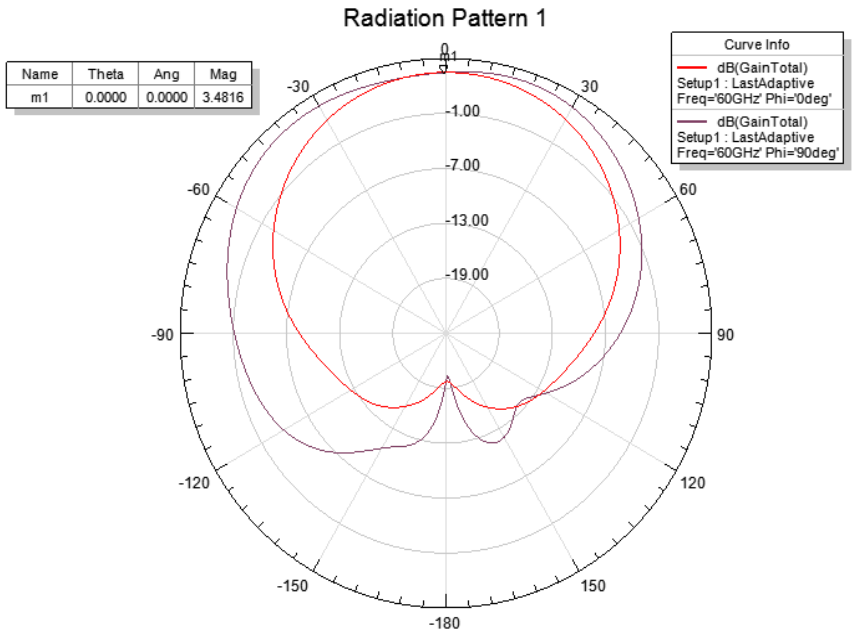

Fig 4.8: Simulated Radiation pattern for antenna design II (Gain = 3.48dB at 60 GHz)

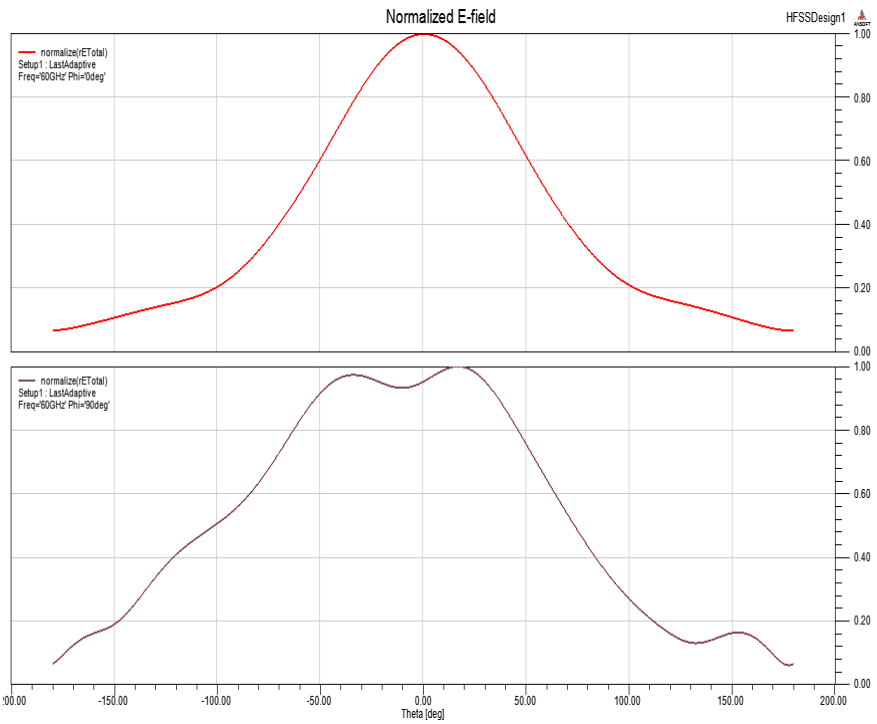

Fig 4.9: Simulated Normalized E for antenna design II

4.3.3 Design III

This design is same as design II, but the only difference is that the CPW feed line is being increased for the purpose of properly feeding the dielectric lens in the middle. The design parameters of the antenna are listed in table 4.4.

Rogers RT/Duroid 5880	
Permittivity (ε_r)	2.2
Loss Tangent (LossD)	0.0009
Substrate Thickness (h)	0.381 mm
Patch Dimensions	
Length (L)	1.3 mm
Width (W)	1.8 mm
CPW Dimensions	
CPW feed Length	10.1 mm

Table 4.4: Design Parameter for Roger RO4350 substrate

It can be seen that now the length of the CPW feed line is longer. The effect of this extra line is that there are more losses which reduces the gain and also the bandwidth of the antenna.

Simulation Results

The simulation results of design III are shown in fig 4.10 and 4.11. The return loss shows that the simulated bandwidth of antenna has decreased to 2 GHz and the antenna is resonating at 60.5 GHz. The radiation pattern shows the maximum gain obtained is approximately 2 dB at the broadside direction.

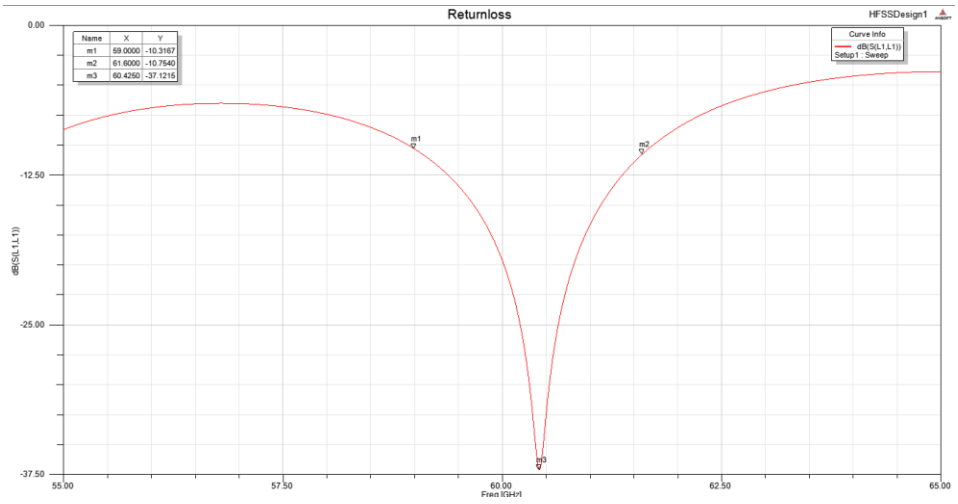

Fig 4.10: Simulated return loss for antenna design III (BW = 2GHz)

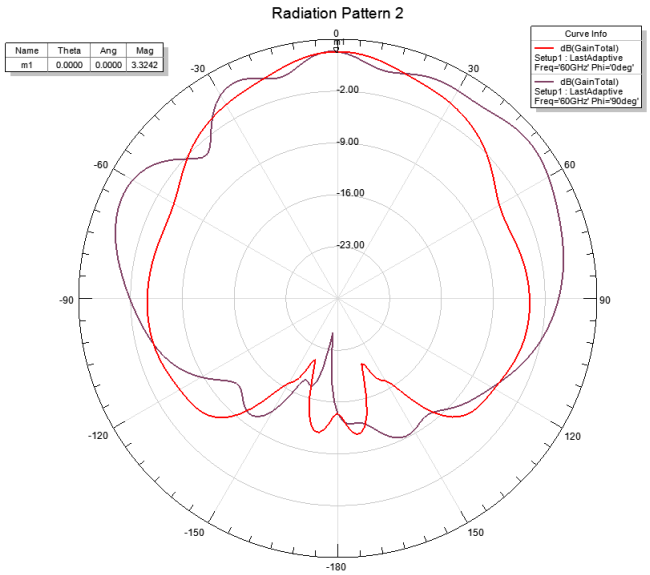

Fig 4.11: Simulated Radiation pattern for antenna design III (Gain = 3.3dB at 60 GHz)

4.4 Fabrication of Single Patch Antenna

The antennas have been fabricated in CTTC laboratory in its Fabrication workshop where single or double-sided printed circuit boards (PCB) for rapid prototyping are manufactured. The equipment used for the fabrication of antennas is LPKF ProtoMat C100 HF (shown in Fig 4.12). It is a milling and drilling plotter system to make double-sided printed circuit boards. LPKF plotters have a wide variety of milling tools. These tools remove copper from board material by applying precision tooling to create isolation paths as small as 100 µm (4 mils) and copper rubout areas as large as required. This equipment is Chemical-free through-hole plating process for single and double-sided printed circuit boards.

Fig 4.12: LPKF Proto-laser Machine

The process of fabrications involves first converting the HFSS designs files into Auto cad files. These files are required to work on the LPKF photo-laser software that operates the LPKF machine and allows to print the design on the copper-substrate sample on both sides thus allowing the double sided PCB circuit prototype manufacturing. However in this thesis only upper side of the antenna was printed on the sample. The top view and bottom view of the antenna is shown in Fig 4.13.

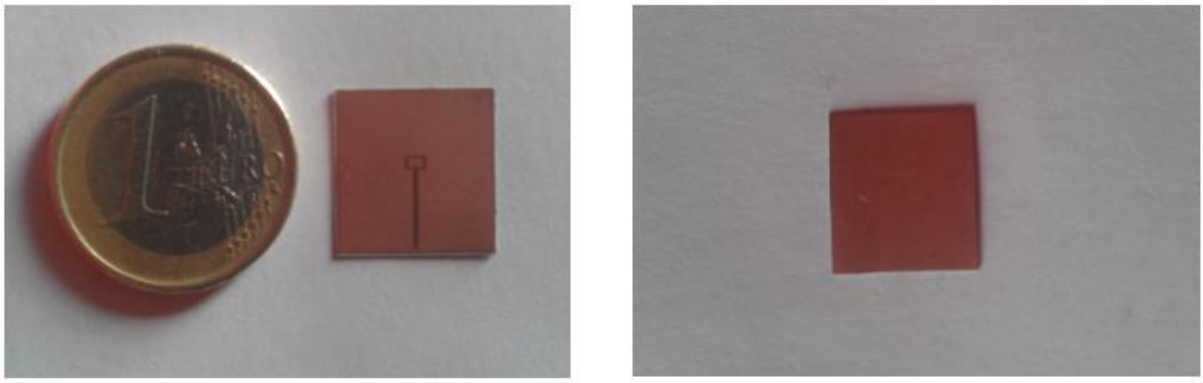

Fig 4.13: Rectangular Patch Antenna Prototype (a) Top View (b) Bottom View

The Laser machine make the contour lines on the substrate for the areas from where the copper is to be removed. Then using the laser it hatches the copper from the unwanted areas and at the end with the help of suction machines all the copper is removed from the contour lines. Since the laser machines precision is 100 um but the gaps in the given design of the antenna are 80 um thus the fabrication was a difficult process for this antenna. However by changing different parameters like power of the laser, repetition and delay time etc, it was possible to design the antenna with better removal of copper and better precision.

4.5 Measurement Results

For the measurements of the antenna, a Cascade Microtech system consisting of probe station with GSG probe that is connected to the Microwave Network Analyzer (VNA) model N52278 which has the frequency range of 10MHz to 67GHz. This system is being used to calculate the S11 parameter i.e. return loss of the fabricated antennas. Fig 4.14 shows the whole probe station.

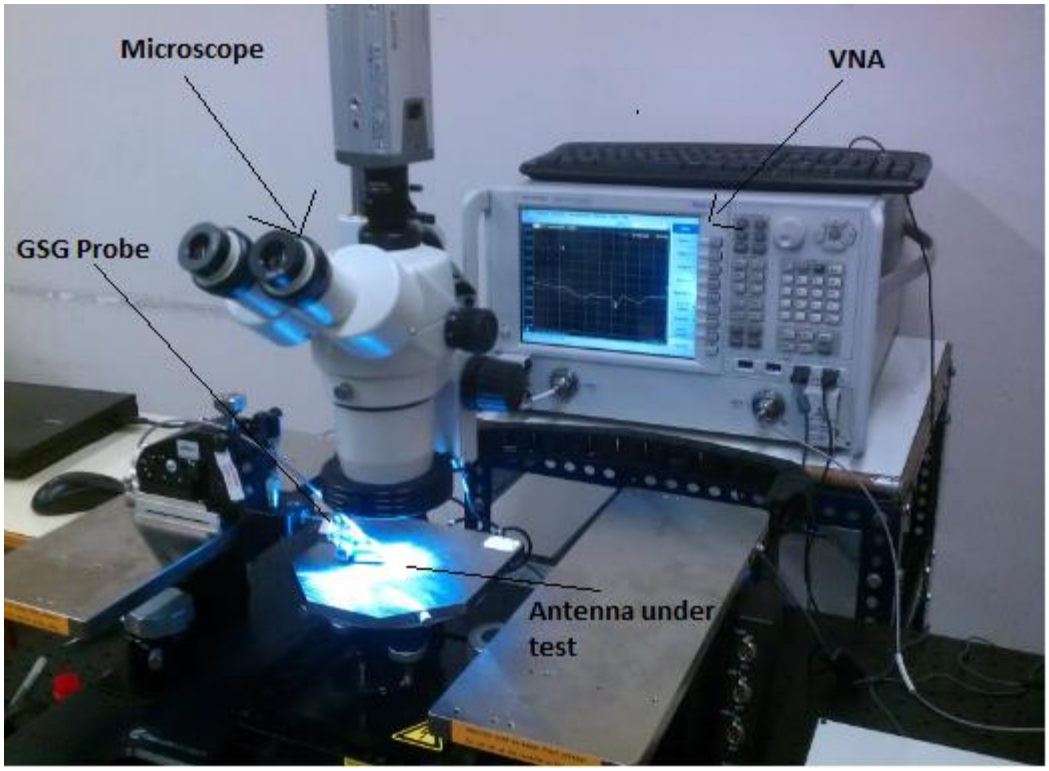

Fig 4.14: Cascade Microtech Probe system for the measurement of S11 Parameter of the Antenna Prototype

Design I: The measured and simulated S11 parameter results of the Design I have been compared in Fig 4.15 and the bandwidth comparison is shown in table 4.5.

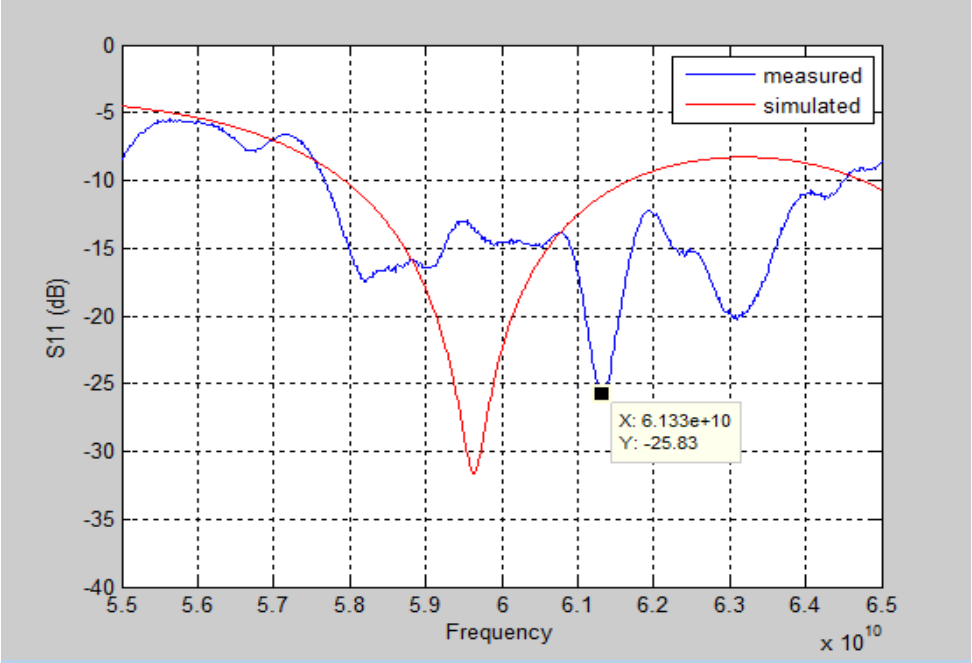

Fig 4.15: Simulated and measured S11 parameter Results of design I

	Simulated		Measured	
Bandwidth	58 GHz to 61 GHz	3 GHz	57.2 GHz to 62.92 GHZ	6 GHz

Table 4.5: Comparison between Bandwidths of design I

Design III: The measured and simulated S11 parameter results of the Design I have been compared in Fig 4.16 and the bandwidth comparison is shown in table 4.6.

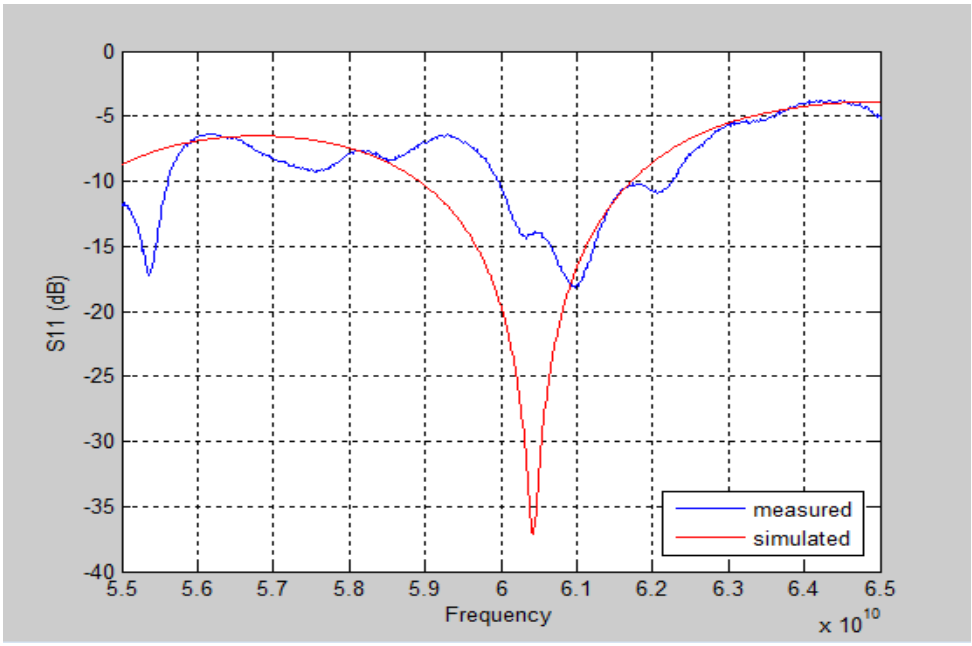

Fig 4.16: Simulated and measured S11 parameter Results of design III

	Simulated		Measured	
Bandwidth	57 GHz to 62 GHz	2 GHz	59.8 GHz to 63.5 2GHZ	2 GHz

Table 4.6: Comparison between Bandwidths of design III

The comparison shows that the resonant frequency in both the designs has shifted towards the higher frequencies and bandwidth is more in measured results. However these results are acceptable because they are in the required specifications.

The radiation pattern measurements are obtained from the measuring systems that is explained in detailed in next chapter. The radiation patterns of the designs I and design III are shown in fig 4.17 to 4.20 respectively.

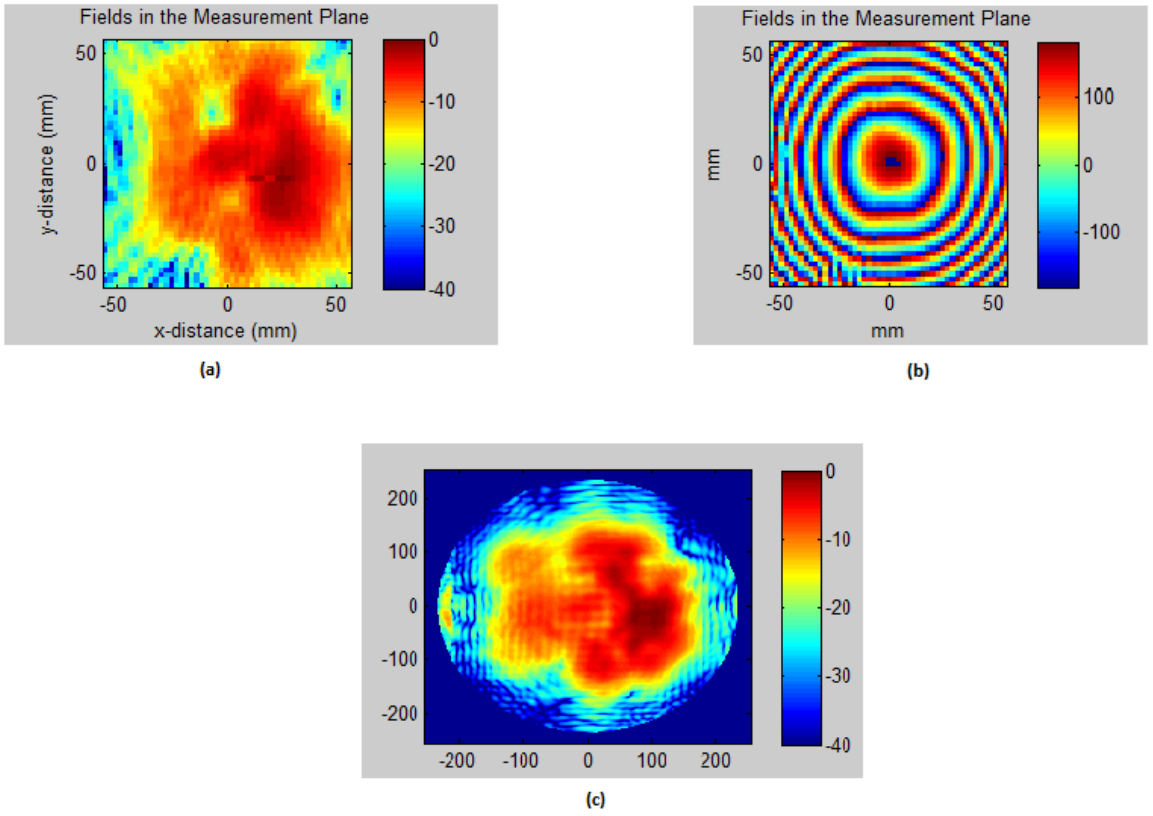

Fig 4.17: Fields in the Near Field Measurement Plane (a) mag dB (b) angle phase (c) on wider grid for Design I

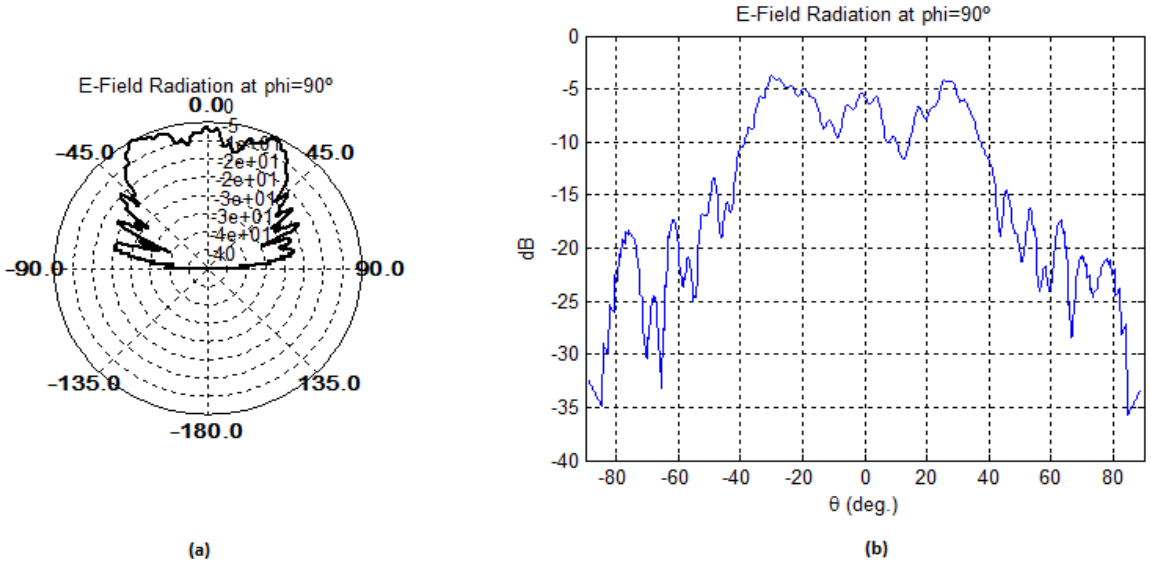

Fig 4.18: E-Field Radiation Patterns for design I at phi = 90 (a) Polar Plot (b) Rectangular Plot

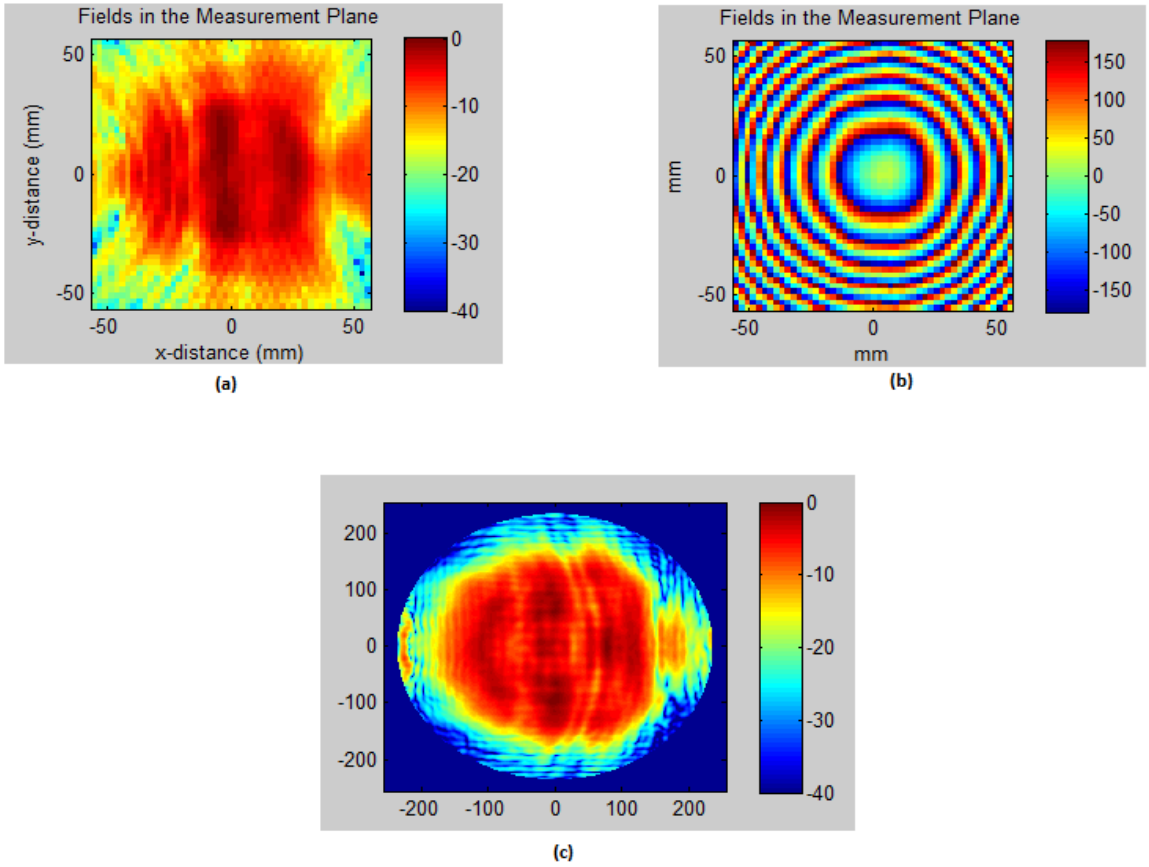

Fig 4.19: Fields in the Near Field Measurement Plane (a) mag dB (b) angle phase (c) on wider grid for Design III

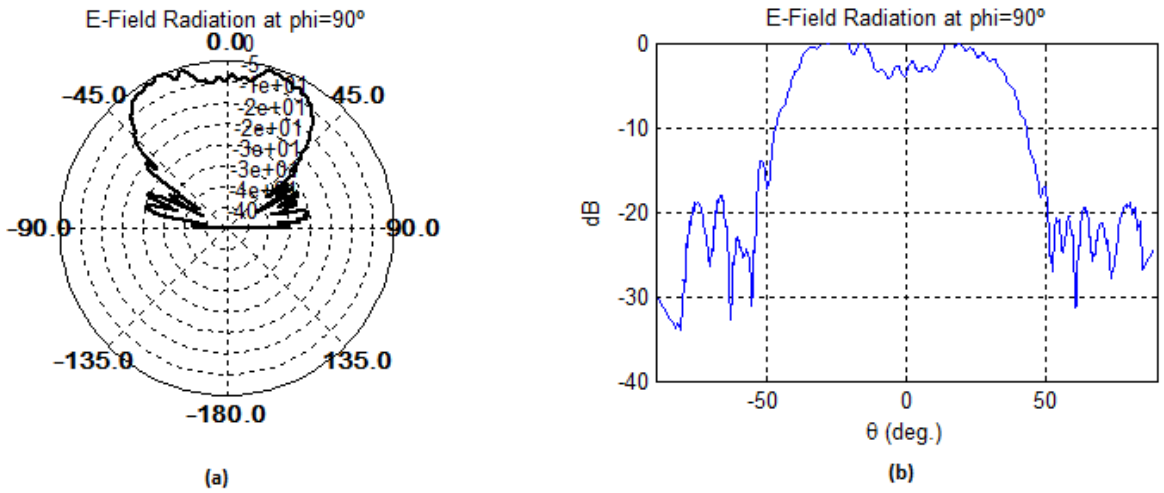

Fig 4.20: E-Field Radiation Patterns for design III at phi = 90 (a) Polar Plot (b) Rectangular Plot

4.6 Patch Antenna as Feed to Dielectric Flat Lens

The dielectric flat lens designed in [1-4] has been re-designed here in HFSS and is simulated with the single patch antenna presented in the previous sections. All the design specifications of the dielectric flat lens are taken from [4.1]. The design in HFSS simulator is depicted in fig 4.21.

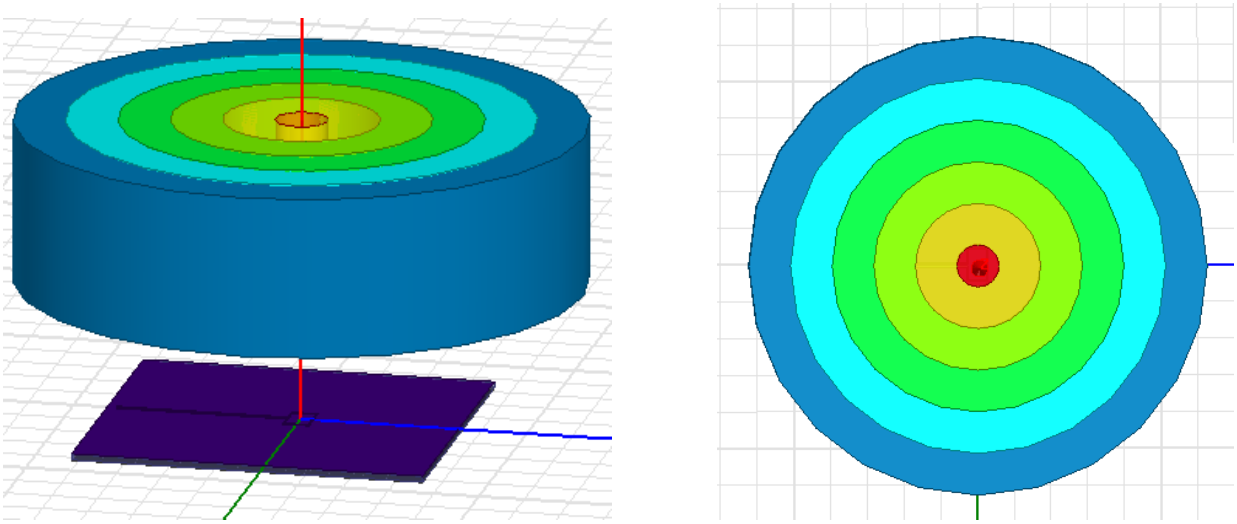

Fig 4.21: Dielectric Flat lens on Top of the Single Patch Antenna, Left: Side View, Right: Top View

In order to obtain the beam scanning from the dielectric flat lens, a total of 5 simulations has been performed by changing the position of the feed patch antenna along x-axis with an increment of 2mm.

The positions along x-axis at which the dielectric flat lens is fed are 0, 2mm, 4mm, 6mm and 8mm. The simulated results of the Gain radiation patterns are shown bellow

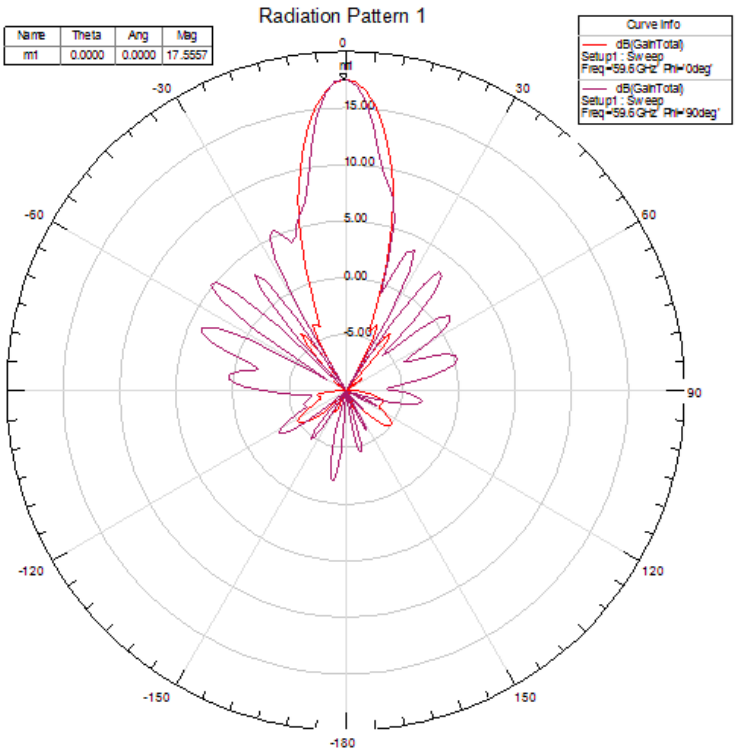

Fig 4.22: For the Patch Position at origin (17.5 dB gain at O°)

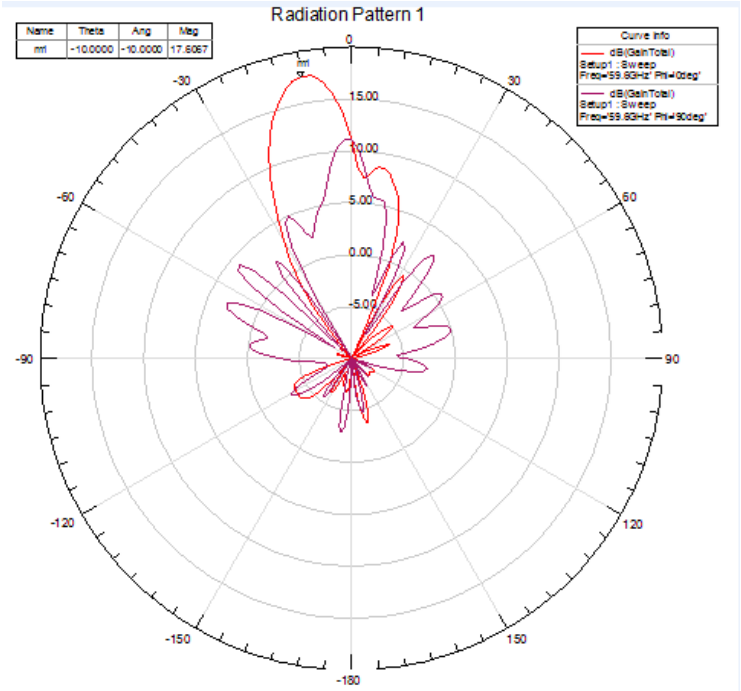

Fig 4.23: For the Patch Position at x = 2mm (17.6 dB gain at -1O°)

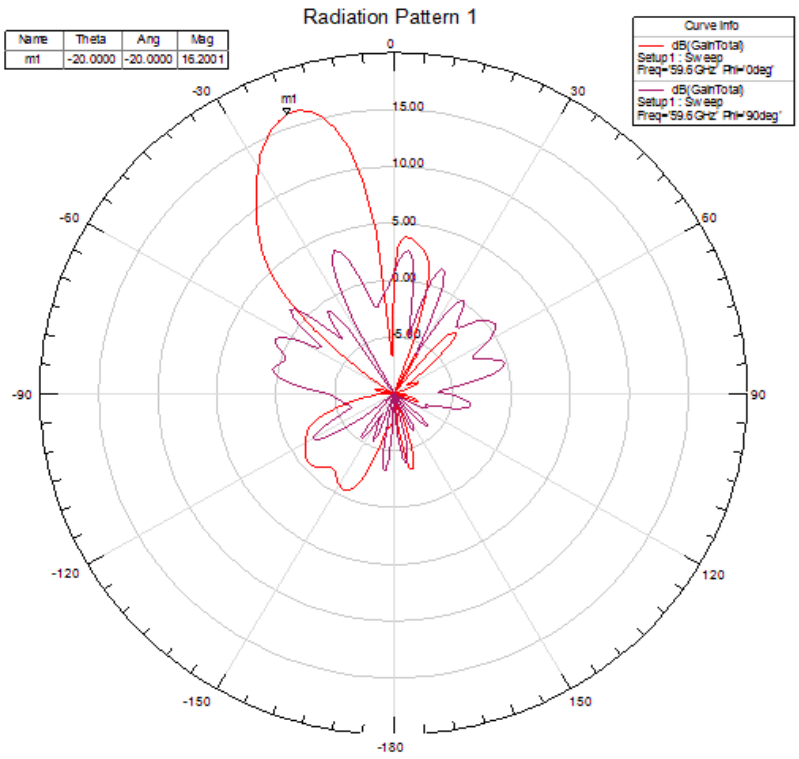

Fig 4.24: For the Patch Position at x = 4mm (16.2 dB gain at -2O°)

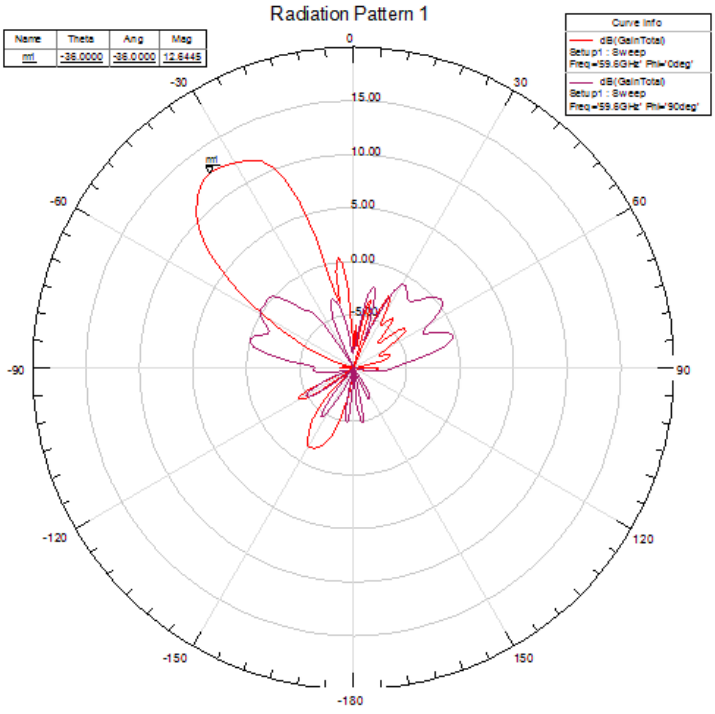

Fig 4.25: For the Patch Position at x = 6mm (12.6 dB gain at -36°)

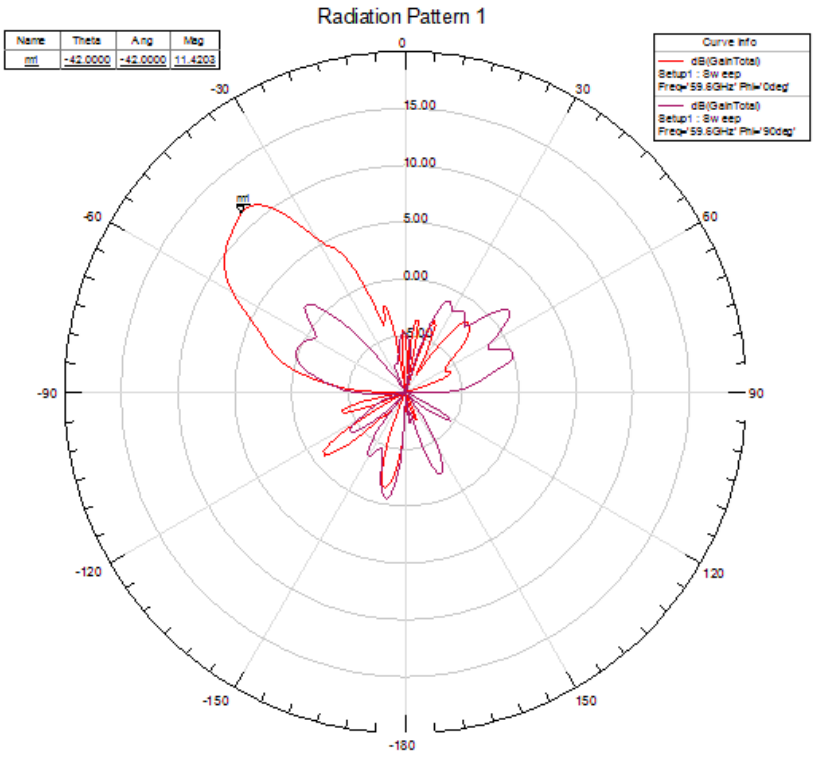

Fig 4.26: For the Patch Position at x = 8mm (11.4 dB gain at 42°)

Due to the symmetry of dielectric flat lens, the same radiation patterns would be obtained when the patch positions is -2mm, -4mm, -6mm and -8mm. Thus with the patch antenna as feed, the dielectric flat lens performs the beam steering from -40° to +40°. Also the patch is placed at the focal point (6.25mm) of the dielectric lens. Table 4.7 shows the overall performance results obtained.

Feeding Position (mm)	Gain (dB)	Steering Angle (°)
0	17.5	0
± 2	17.6	10
± 4	16.2	20
± 6	12.6	36
± 8	11.4	42

Table 4.7: Overall Performance Results

So now the aim of the rest of the project is to replace this single patch antenna with the Antenna array that performs beam steering with in the entire band of interest (57 GHz to 64 GHz) and instead of changing the positions of the patch, the lens can be feed at different places by just changing the frequency of feeding.

5. Series Fed Linear Patch Antenna Array Design and Results

5.1 Introduction

In the second part of the project, Linear Array has been designed using the patch antenna designed in the first part as the single element of the array. To achieve the beam steering capabilities depending on the frequency change in the required band, array has been fed in series. The array is required to switch the beam with in the 60 GHz band i.e. 57GHz to 64GHz. The rest of the chapter deals with the design, simulation and measurement of antenna array.

5.2 Design Specifications

For the design of the array, out of the three designs of single patch presented in previous chapter, design I has been chosen which used the substrate Rogers RO4350. The same software HFSS has been used for the designing. The design of the array is shown in fig 5.1. In the figure de is the distance between the elements for the array, L and W are the length and width of the single patch of design I.

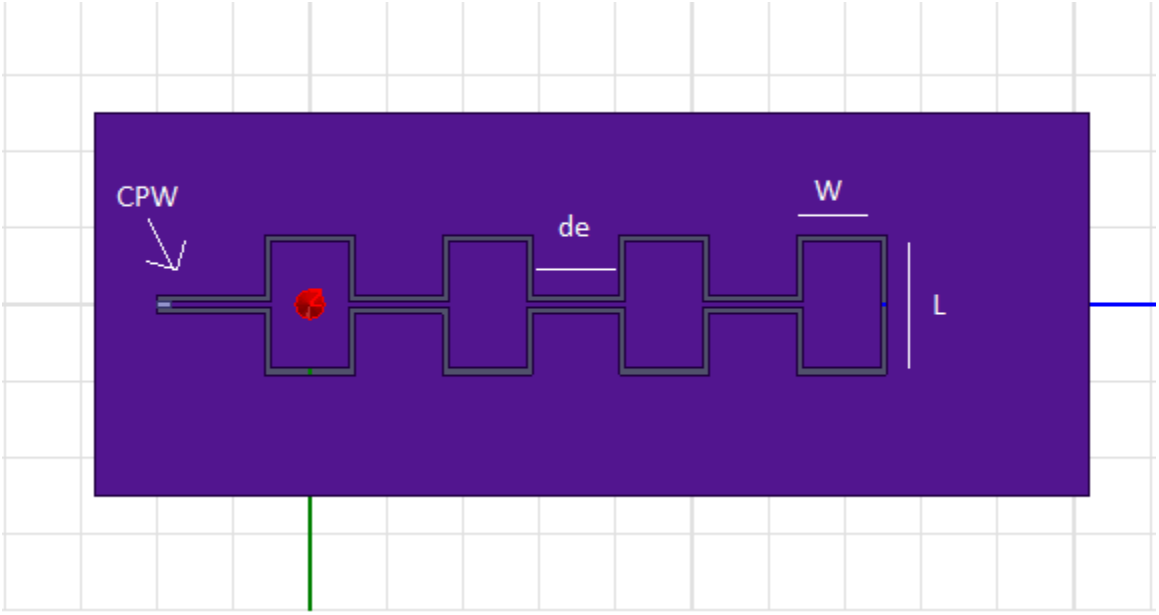

Fig 5.1: Design of a Series Fed Linear Patch Array

Same as the single patch, array is also required to resonate at 60GHz. The distance between the array elements is an important consideration and it has to be selected in order to obtain broadside radiation pattern at 60 GHz. Moreover the CPW feed gap has the same dimension as in the single patch design because of the same reasons.

5.3 Design of Series Fed Linear Patch Antenna Array

A 4×1 linear patch array for 60 GHz applications has been designed by performing the steps given in fig 5.2. As discussed before, the array is series fed to make frequency sensitive and to obtain beam steering over the entire band of interest.

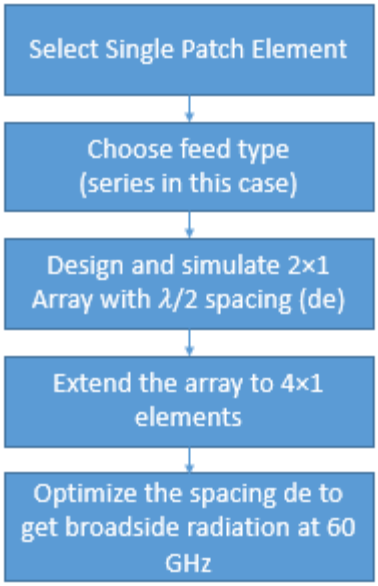

Fig 5.2: Steps followed to design the 4×1 Linear Patch Array

By performing multiple simulations, the de is selected to be 0.26 λ (≈λ /4) which gives the main beam direction into broadside of the array at 60 GHz. Now by changing the frequency from 60 GHz to 57 GHz, the electrical length of de changes at this new frequency. This change in length causes change in the phase of each element i.e. given by $e^{-j\beta de}$ thus causing the main mean to tilt to right direction. Similarly by changing frequency from 60 GHz to 63 GHz, the beam direction is tilted to left. Thus in this way we get the beam steering only by changing the frequency. The design parameters of the array are shown in the table 5.1.

Design Parameters		
Length of Single element	L	1.1 mm
Width of single element	W	1.65 mm
Substrate thickness	H	0.254 mm
Distance between elements	De	1.29 mm

Table 5.1: Design Parameters for the Series-Fed Linear Array

5.4 Simulation Results

First the array is being simulated at 60 GHz and the simulation results are shown in fig 5.3, 5.4, 5.5 and 5.6. The array resonates at 58.8 GHz and the maximum radiation is at broadside (0°) with a gain of 5.2 dB. The SSL is -9 dB.

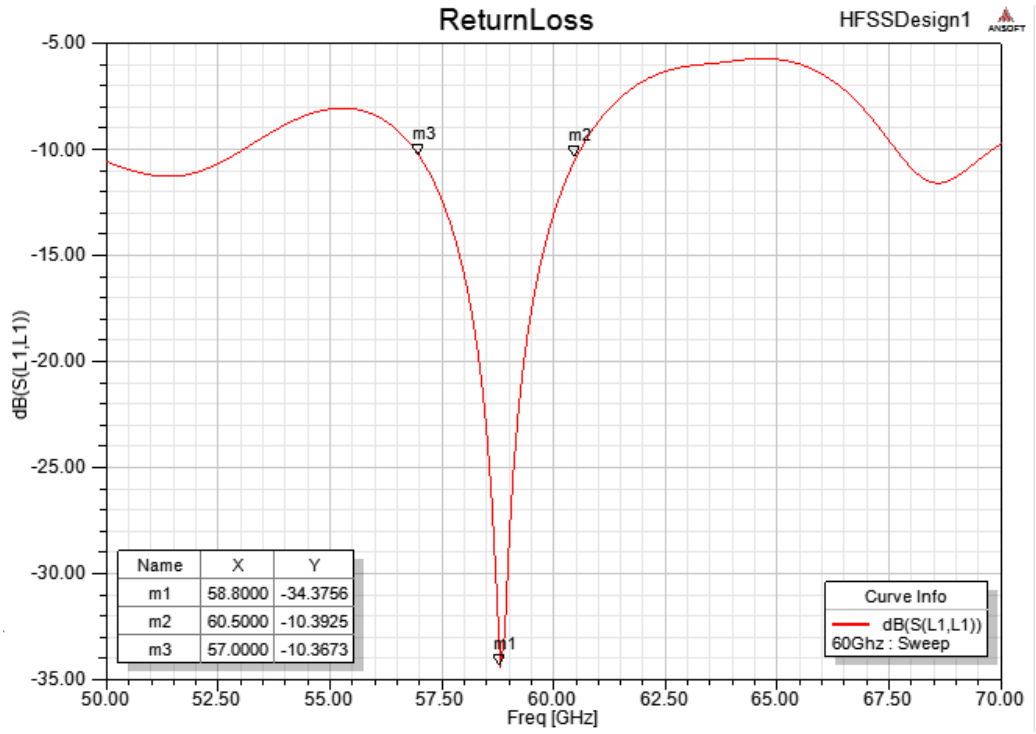

Fig 5.3 Return Loss at 60 GHz (resonates at 58.8 GHz)

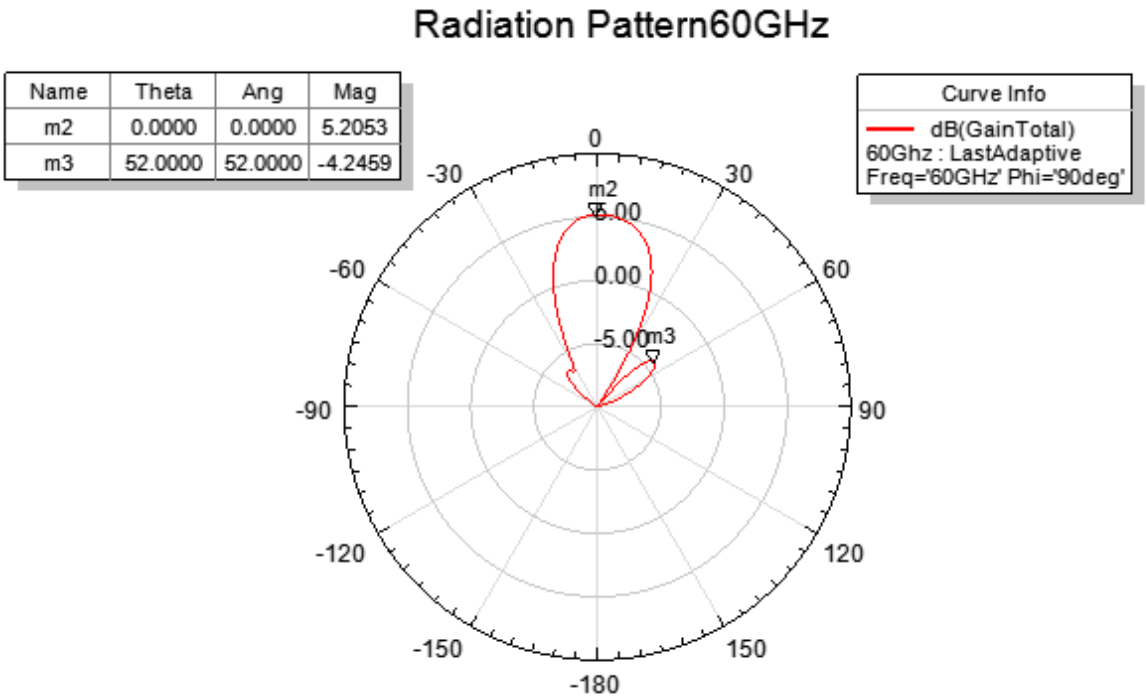

Fig 5.4: Radiation Pattern at 60 GHz (Gain 5.2 dB with SSL -9dB)

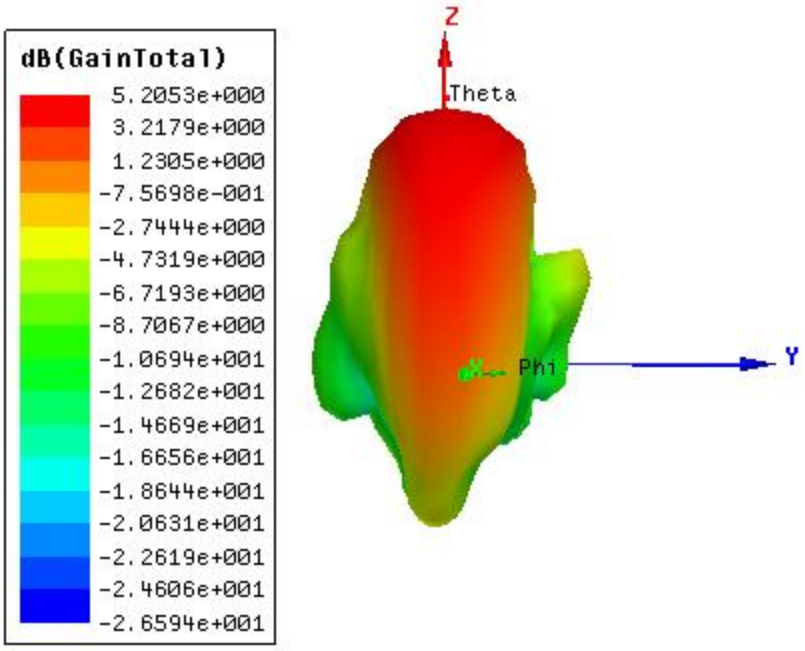

Fig 5.5: 3D Polar Plot

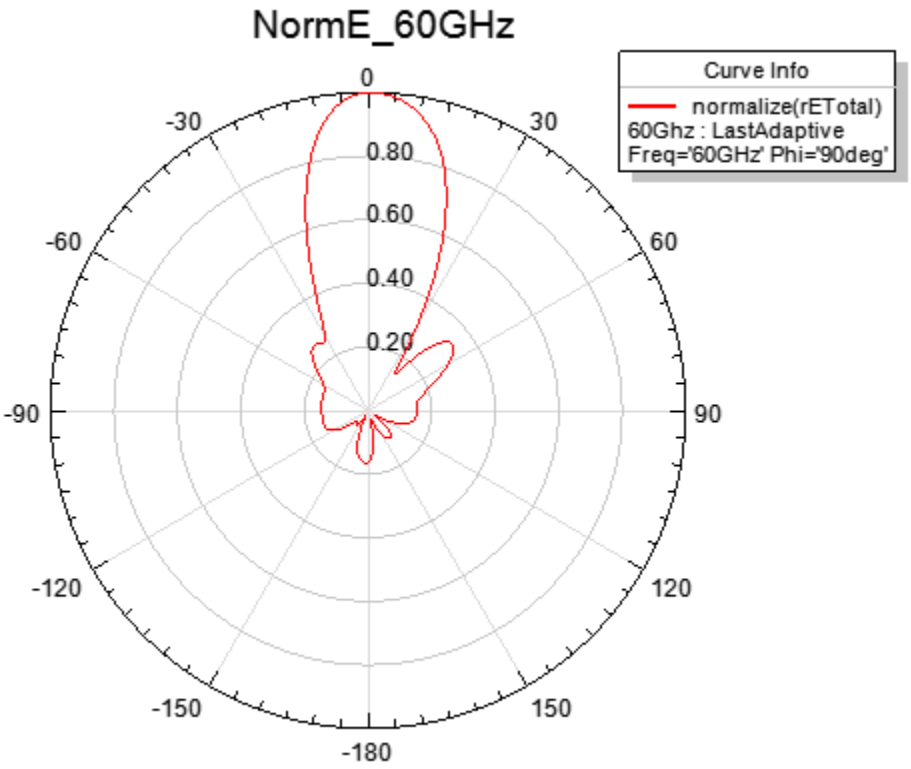

Fig 5.6: Normalized E- Field Radiation Pattern at 60 GHz

After obtaining the results for the 60 GHz, now the solution frequency is changed from 57 GHz to 64 GHz (which is the V-Band for WPAN application) with a step of 1 GHz. It has been observed that the beam steering of ±10° was achieved with maximum gain of 7 dB and SSL of ≈ 9dB. The Normalized E-Field radiation patterns of the frequencies has been shown in fig 5.7. The gain patterns are shown in fig 5.8.

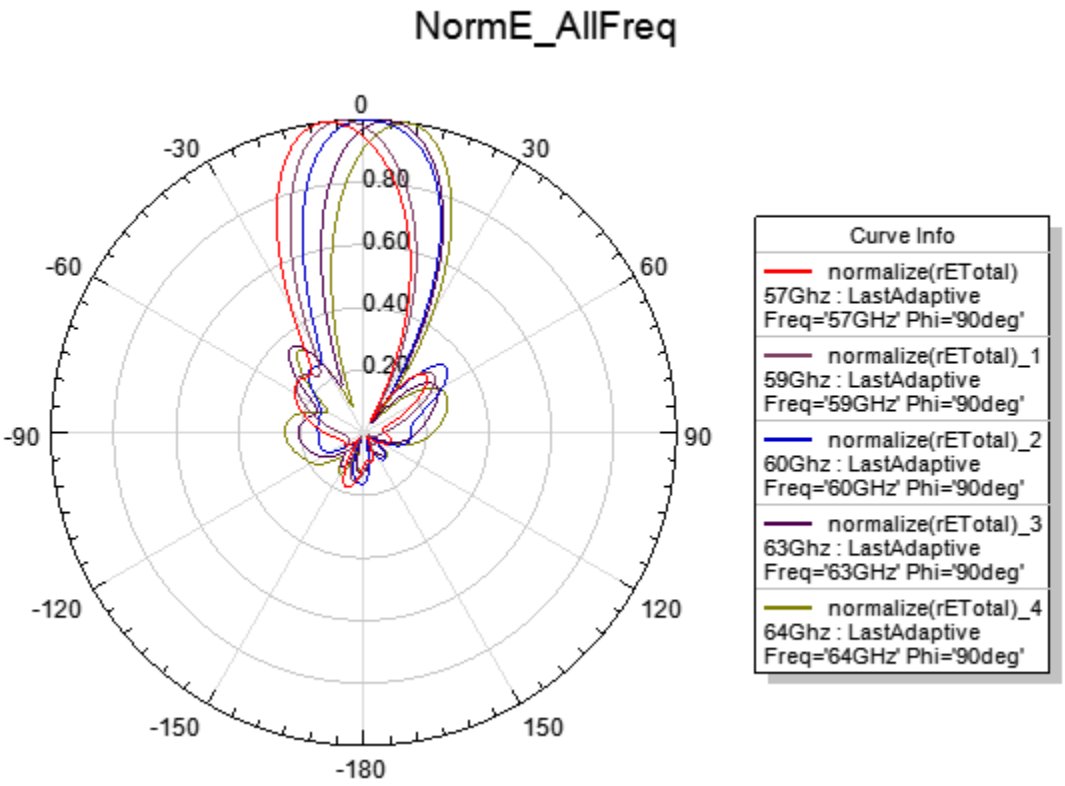

Fig 5.7: Normalized E-Field Radiation Pattern for each frequency

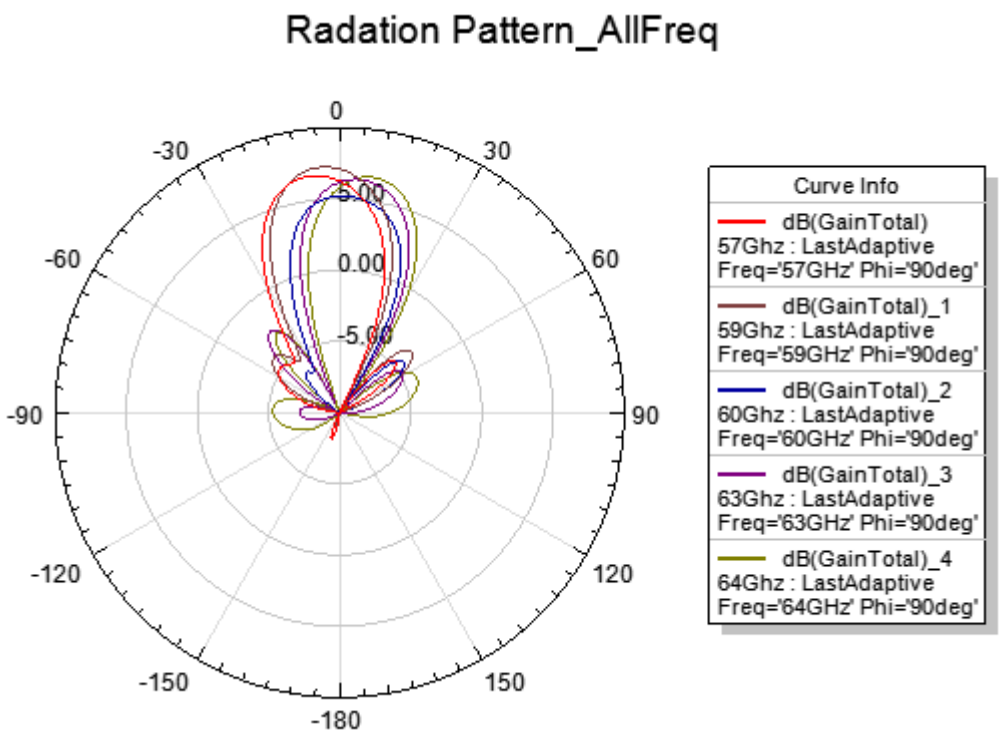

Fig 5.8: Gain Radiation Patterns for each Frequency

A comparison of the return loss, gain, SSL and angle of beam direction of all the simulated frequencies have been made in table 5.2.

Frequency (GHz)	S11 (dB)	Gain (dB)	SSL (dB)	Angle of Direction
57	-11.01	6.72	11	-10°
58	-11.97	6.31	10	-10°
59	-10.75	7.27	10.5	-5°
60	-13.01	5.20	9	0°
61	-29.06	6.98	9.5	+2°
62	-12.57	5.50	7.5	+5°
63	-12.83	6.40	9	+6°
64	-8.61	6.49	9	+10°

Table 5.2: Comparison of S11 parameter, Maximum Gain, SSL and beam angle at each of the frequencies

Note that in the Normalized E-field and gain patterns few of the frequencies in between have been left out because of the similar pattern and to get more clarity of the beam steering.

5.5 Fabrication of Linear Array

The Linear array has been manufactured by the process of photolithography. Photolithography is a process that is used for micro fabrication. It plots pattern on parts of thin films or substrate using light to transfer geometric patterns from a photomask to a light-sensitive chemical 'photoresist' material on the substrate. With the process of series of chemical statements, an exposed pattern can be either engraved

on the photoresist material or desired pattern can be formed by decomposition of new material. This manufacturing process for fabricating the linear array has been carried out in the laboratories of D3 building in department of Signal theory and Communications at UPC, using standard techniques of photo plotting. However the block diagram and the brief description of the steps carried out for photolithography are presented in Appendix B.

After the manufacturing of array prototypes, the top and bottom view of the array has been shown in fig 5.9 and 5.10.

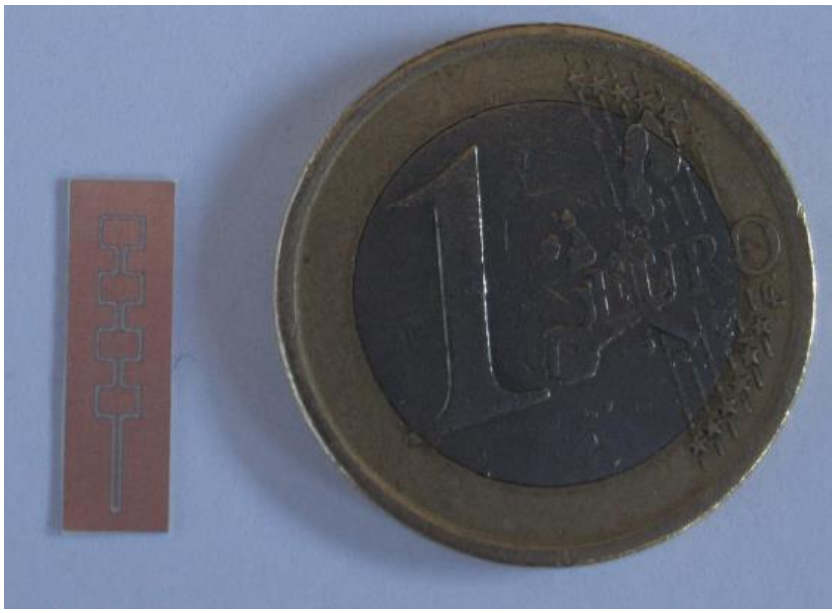

Fig 5.9: Top View of the 4 element Antenna Array

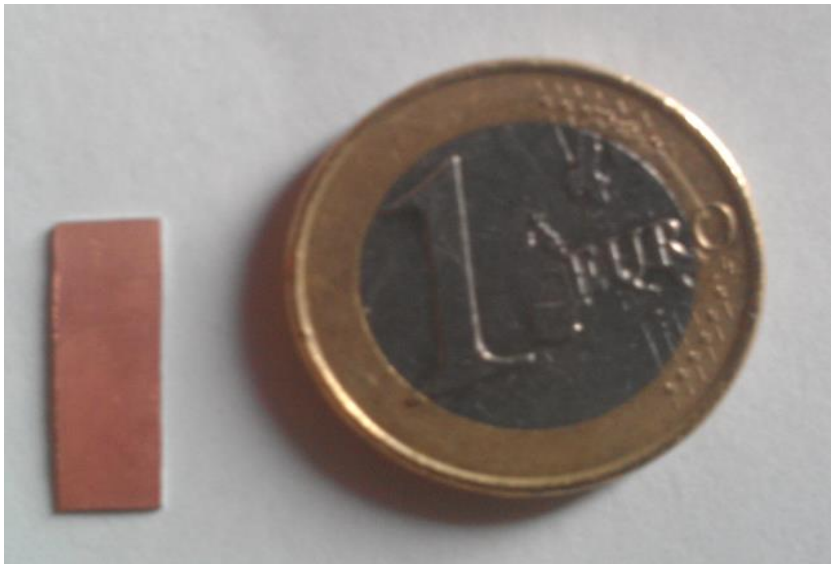

Fig 5.10 Bottom view of 4 element Antenna Array

5.6 Measurement System and Results

After establishing all the prototypes of antenna array, now the radiation properties of array has been analyzed in the Antenna Lab in D3 building of UPC.

5.6.1 Measurement of S11 Parameter

At first the measurements for the S11 parameter of the prototypes have been obtained from the Cascade Microtech that has been used for the measurement of the return loss of single patch antenna and has already been discussed in previous sections. Fig 5.11 shows the comparison between the simulated return loss (S11) and measured one and fig 5.12 shows the setup of the array where it is being fed by GSG probe.

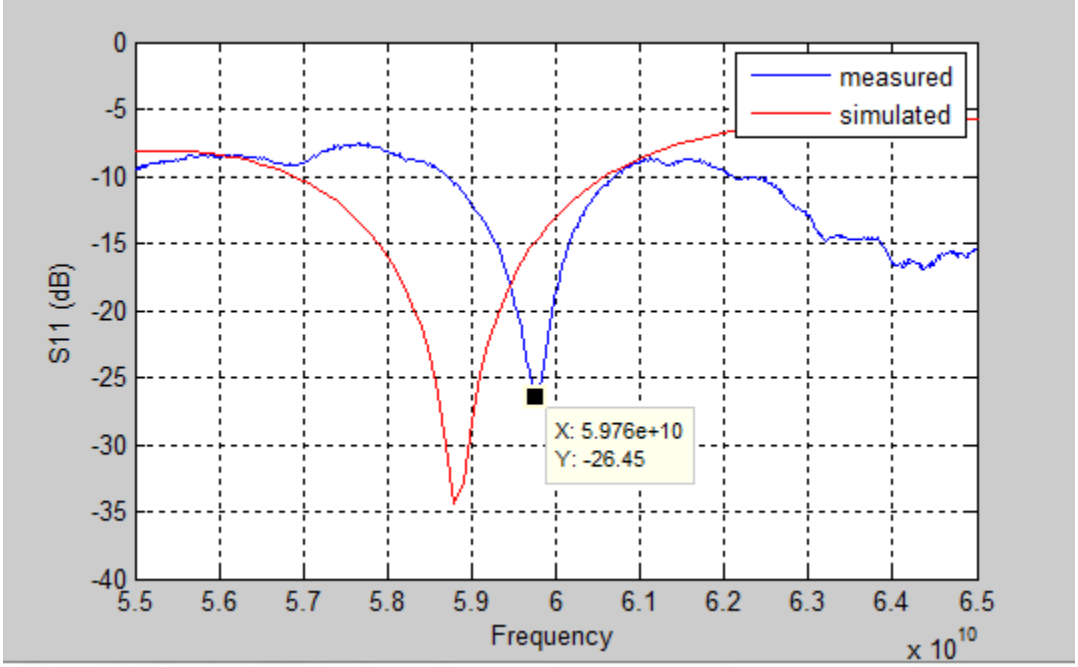

Fig 5.11: Simulated and measured S11 parameter Result for Linear Array

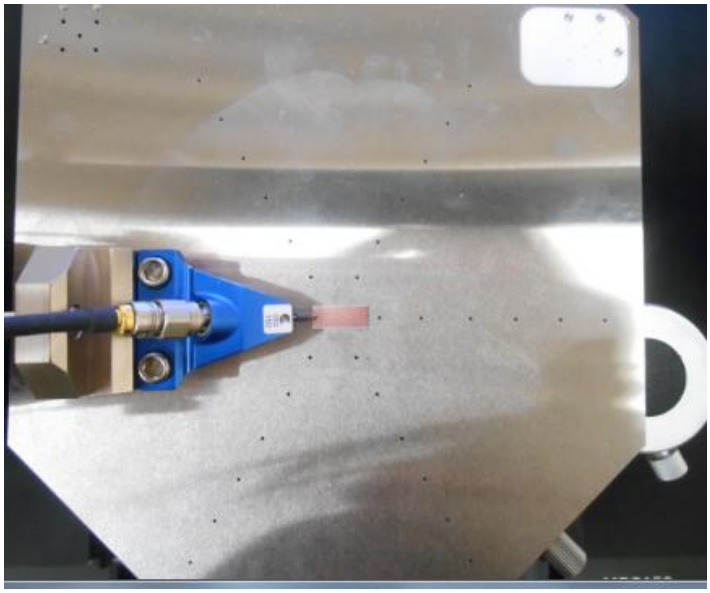

Fig 5.12: Feeding the Antenna Array with GSG 150um pitch Probe

5.6.2 Measurements of Radiation Patterns:

For measuring the E-Field radiation patterns of antenna array at a frequency of 60GHz, a 2D Near-Field measuring system has been built in Antenna Lab of UPC. A block diagram of measurement configuration is shown in fig 5.13 which presents all the components required for measurements. It is composed of:

- an Agilent VNA (Vector network analyzer) N52278
- two precision linear stages to perform the 2D scan (X-Y movements)
- a stage controller to control stages
- an open waveguide WR15 as a receiver probe
- One GSG 150um pitch probe to feed the antenna array

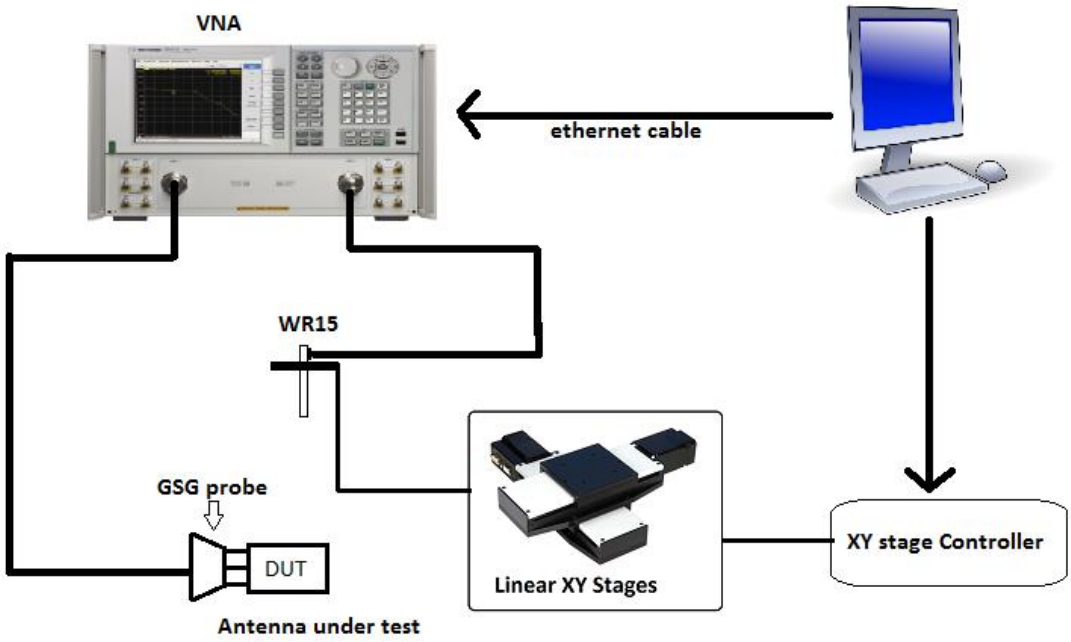

Fig 5.13: Block Diagram of the measurement System for Radiation Pattern in V-Band (57 GHz to 60GHz)

Measuring Procedure: The antenna is placed on the Cascade Microtech system and is fed with the 150um pitch GSG probe which is then connected to the VNA port 1. To the VNA port 2, an open waveguide WR15 is connected. Both the GSG probe and WR15 are connected using the cables that work up to 67GHz. The linear x-y stages allow the WR15 to scan above the antenna in x and y directions. The concept of 2D scan includes keeping first y constant and moving WR15 in x direction in steps and capturing all the E-Field values at these points. Then take a step forward in y-direction and repeat the process. In this way with the help of these stage movements, the 2D E-field calculation above the antenna are captured in the VNA as S21 parameter. This process is shown in fig 5.14. These S21 values from VNA are then transferred to the computer through Ethernet cable. Then using these values in Matlab routines, E-Field radiation pattern in far-field is obtained. Also the x and y stages are controlled by Matlab routines in computer.

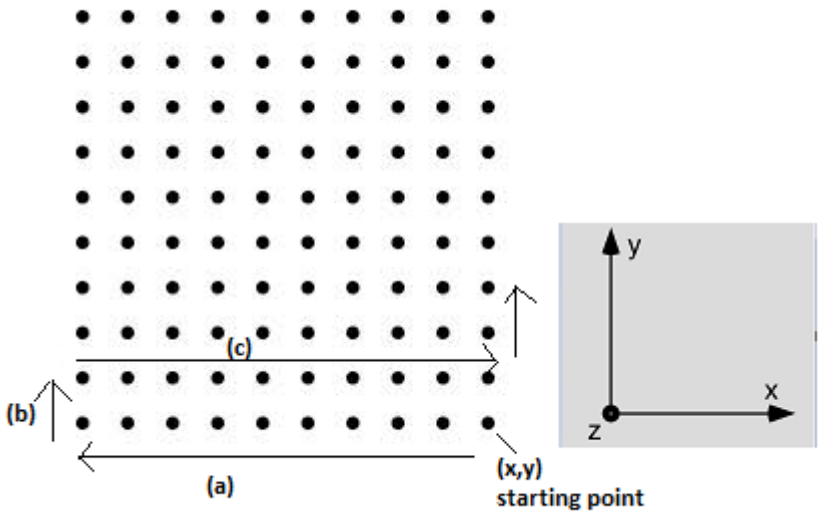

Fig 5.14: Positions of the WR15 for 2D Scan by the linear stages. (x,y) is the starting point. (a) At y=1, x is incremented. (b) Then y is incremented (c) x is incremented now in backward direction. Finally the process is repeated.

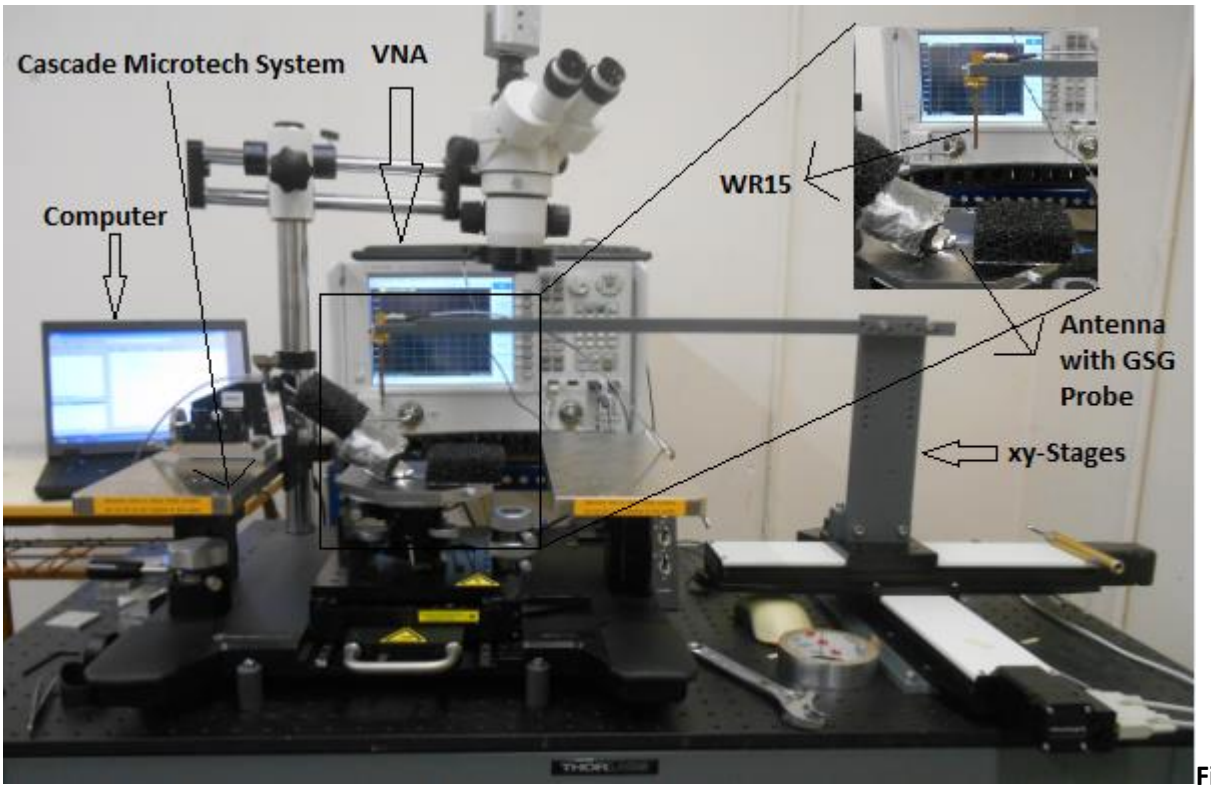

Fig 5.15: 2D Near Field Measurement System at 60 GHz

The absorbers have been used across the probe and around the antenna under test in order to avoid the radiations from the probe and the surrounding elements.

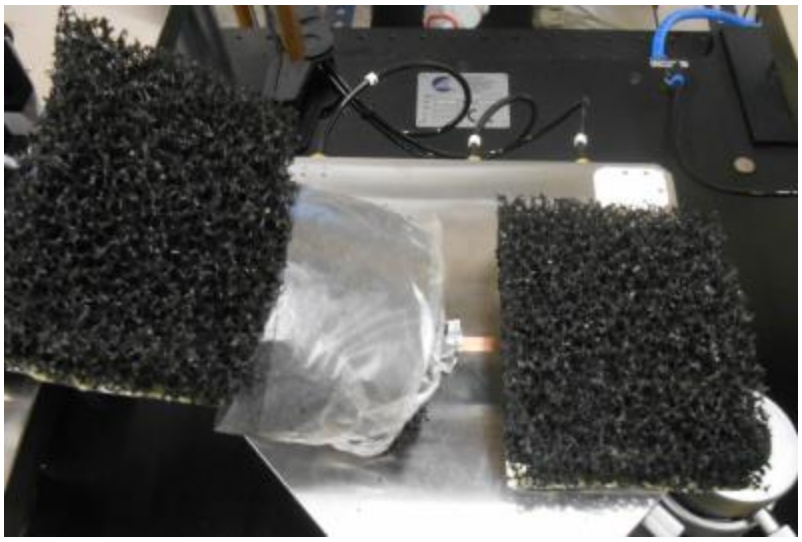

Fig 5.16: Absorbers around antenna array are being used to avoid spurious radiations

The E-Field radiating by the antenna array is been measured in the Near-Field at approximately 40mm from the antenna aperture. The Far-Field radiation patterns are then obtained by using Near-Filed to Far-Field transformations. The real time measurement setup is shown in figure 5.15. The antenna array prototype is fed over a range of 57GHz to 64 GHz, however the results are shown for the frequencies 57, 59, 60, 61 and 63 GHz for more clarity and observation. The corresponding rectangular E-Field radiation patterns are shown in fig 5.17. It can be seen that by increasing the frequency, the main beam shifts along the theta axis from -18° to 0°.

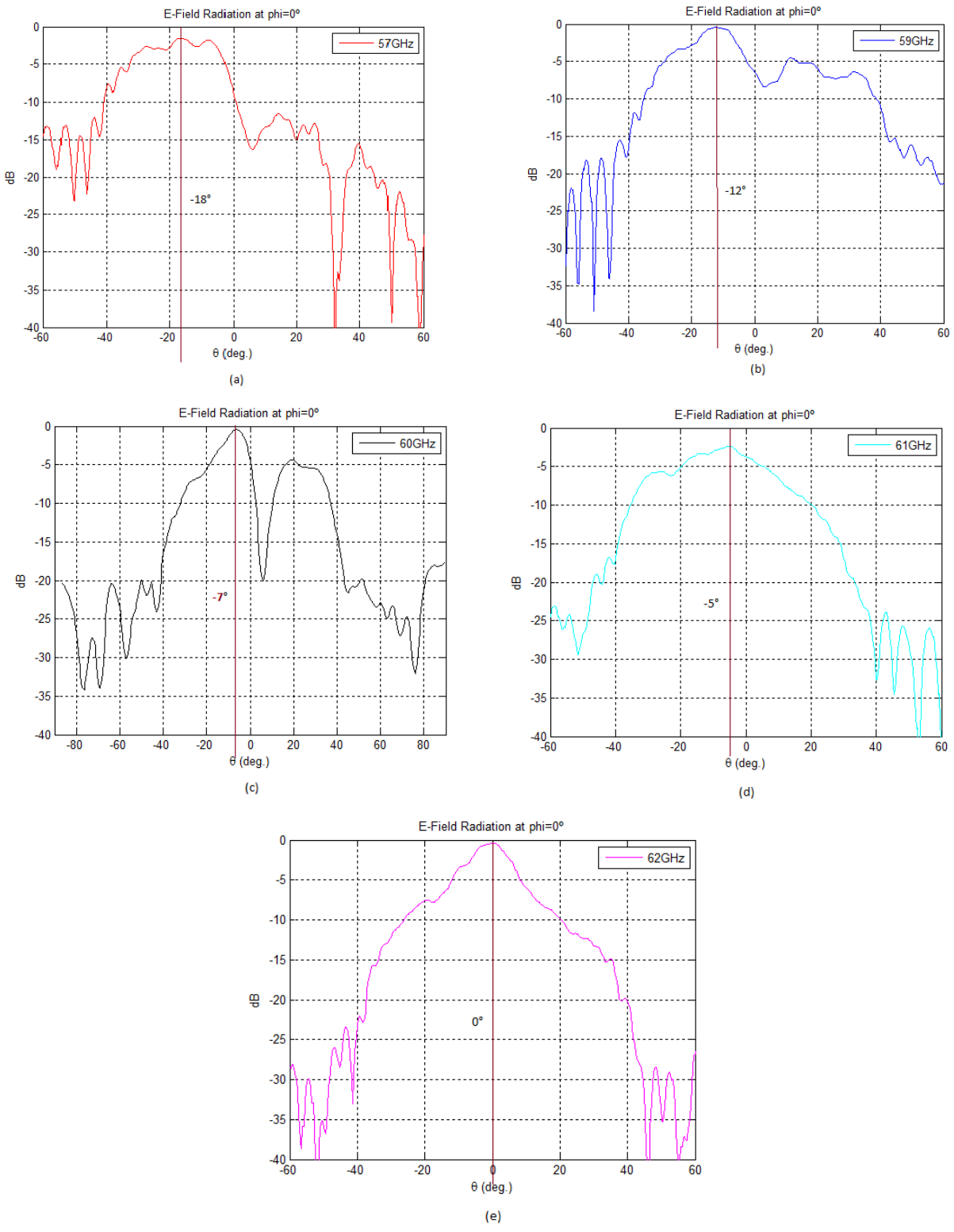

Fig 5.17: E-Field Radiation Pattern at phi = 0° (a) 57 GHz with beam at -18° (b) 59 GHz with beam at -12° (c) 60 GHz with beam at -7° (d) 61 GHz with beam at -5° (e) 63 GHz with beam at 0°

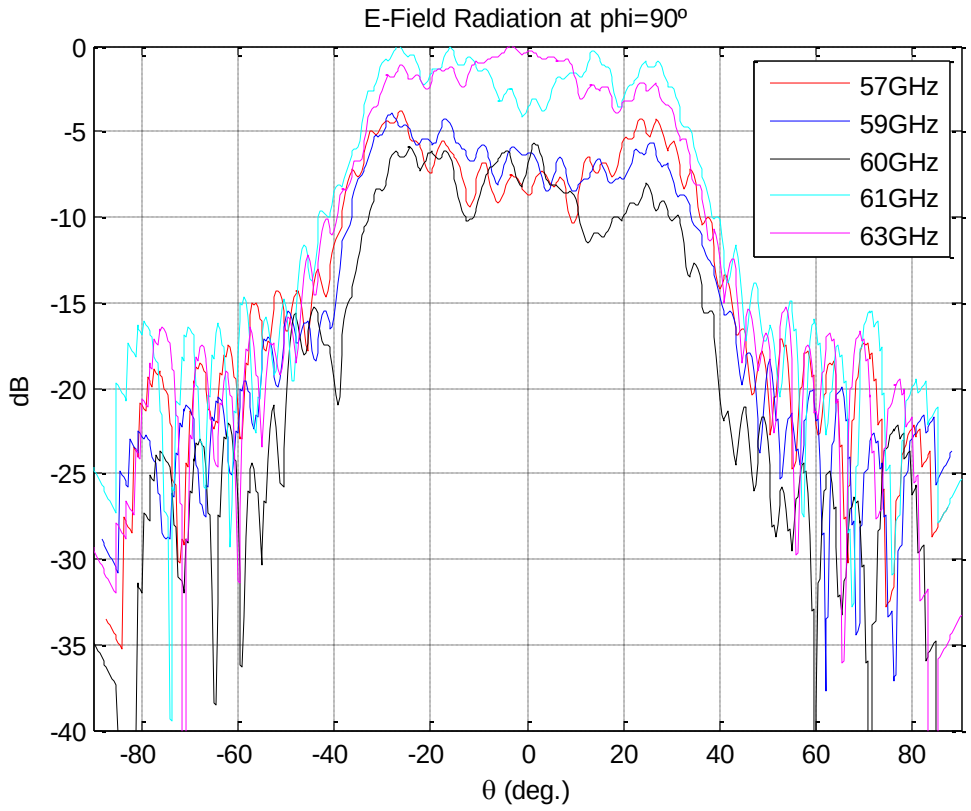

Fig 5.18: E-Field Radiation Pattern at phi = 90°

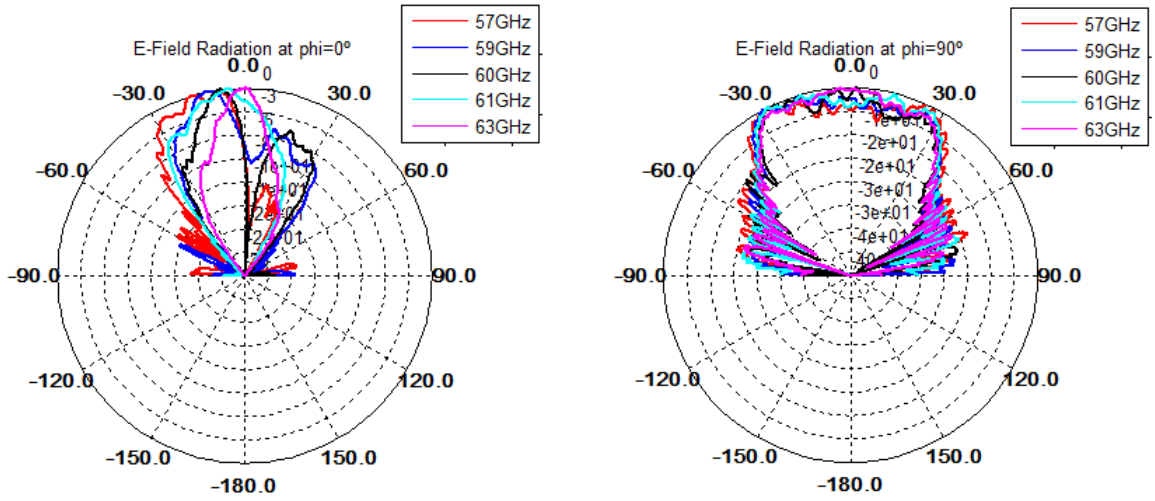

Fig 5.19: E-Field Radiation pattern in polar coordinates (a) phi = 0° (b) phi = 90°

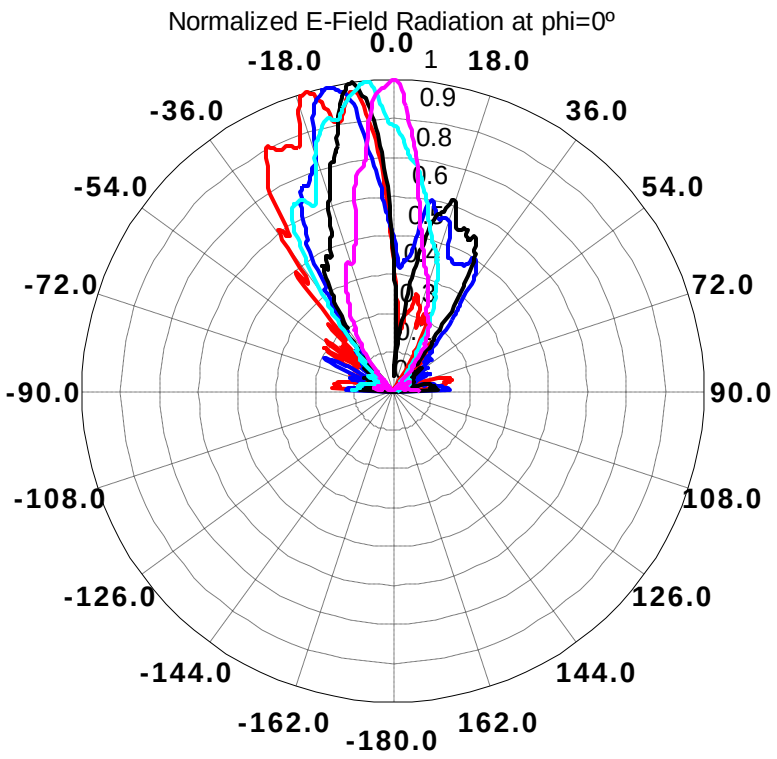

Fig 5.20: Normalized E-Field Radiation pattern at phi = 0°

It has been observed that the measured results from the designed prototypes and the simulation result are different. Their comparison is being made and is presented in Table 5.3.

Parameter	Measured	Simulated
Resonant Frequency	58.9 GHz	59.7 GHz
Beam Steering	-18° to 0°	-10° to 10°
Avg Side Lobe Level	≈9.4 dB	≈ 8.2 dB

Table 5.3: Comparison between Measured and Simulated values of the Linear Antenna Array Design

The measured results are deviated from the simulated one both in the range of scanning and in the SSL. The reason for this deviation is that the array has been manufactured with the process of photolithography which is not a very high precision manufacturing process. In simulation, the gap of CPW feed for the array is very thin but the chemical attack from the manufacturing process caused this gap to increase and reduce the feed line. However this has been verified by performing the simulation of the array with the wider gap and thinner CPW feed line and the result obtained for beam steering are -18° to 0° as obtained with the measured array.

6. Conclusion

In this project a CPW fed Microstrip patch antenna and series fed antenna array has been designed at 60 GHZ for WPAN applications. The single patch antenna has been designed and fabricated to obtain higher bandwidth. In order to obtain higher bandwidth two different substrates has been used in the design. The maximum bandwidth obtained from one of the design is 6 GHz with in V-band (57 GHz to 64 GHz) with the gain up to 3dB.

This single patch is then used to feed the dielectric flat lens. The les was fed at different positions with the single patch which gave the beam steering capability from -40° to +40° over the entire V-band of interest. The patch was placed at the focal point of the dielectric lens.

Later using the single patch antenna, an array is designed to operate in the frequency band of 57 GHz-64 GHz. The purpose of the array is to perform the beam scanning with the shift in the frequency so that the array has the scanning capabilities with the fixed multiple beams which can be selected individually. The beam steering of ±10° has been obtained by shifting the frequency from 57 GHz to 64 GHz.

Appendix A

High Frequency Structural Simulator (HFSS)

Ansoft High Frequency Structure Simulator is a full-wave, FEM-based electromagnetic field solver for simulating arbitrary (3D) structures. HFSS is used to simulate Connectors Waveguides On-chip components Antennas etc and used for parametric sweeps Structure optimization etc.

HFSS is based on a three-dimensional FEM, a frequency domain method (solutions are calculated for each frequency separately). FEM divides the whole model space into small finite elements (triangles or tetrahedral) and represents the field in each subdomain with a local function for the volume of total of *N* sub-domains, the scattered field can be expanded into a series of known basis functions with unknown expansion coefficients. The value of a vector field quantity at points inside each tetrahedral is numerically interpolated from the values at the vertices and the midpoints of the edges. The simulator transforms Maxwell's equations into matrix equations, which can be solved using numerical methods. The simulation time is proportional to *N* (when solved iteratively) or *N*^3 (if system matrix is inverted directly).

The Adaptive Analysis Process (from HFSS help)

An adaptive analysis is a solution process in which the mesh is refined iteratively in regions where the error is high, which increases the solution's precision. You set the criteria that control mesh refinement during an adaptive field solution. Many problems can be solved using only adaptive refinement.

- HFSS generates an initial mesh.
- Using the initial mesh, HFSS computes the electromagnetic fields that exist inside the structure when it is excited at the solution frequency. (If you are running a frequency sweep, an adaptive solution is performed only at the specified solution frequency.)
- Based on the current finite element solution, HFSS estimates the regions of the problem domain where the exact solution has strong error. Tetrahedral in these regions are refined.
- HFSS generates another solution using the refined mesh.
- HFSS re-computes the error, and the iterative process (solve error analysis refine) repeats until the convergence criteria are satisfied or the requested number of adaptive passes is completed.
- If a frequency sweep is being performed, HFSS then solves the problem at the other frequency points without further refining the mesh.

Frequency Sweeps (from HFSS help)

Perform a frequency sweep when you want to generate a solution across a range of frequencies. You may choose one of the following sweep types:

- **Fast:** Generates a unique full-field solution for each division within a frequency range. Best for models that will abruptly resonate or change operation in the frequency band. A Fast sweep will obtain an accurate representation of the behavior near the resonance.
- **Discrete:** Generates field solutions at specific frequency points in a frequency range. Best when only a few frequency points are necessary to accurately represent the results in a frequency range.

- **Interpolating:** Estimates a solution for an entire frequency range. Best when the frequency range is wide and the frequency response is smooth, or if the memory requirements of a Fast sweep exceed your resources.

Excitations (from HFSS help)

Assigning excitations to an HFSS design enables you to specify the sources of electromagnetic fields and charges, currents, or voltages on objects or surfaces.

- Wave port
- Lumped port
- Incident wave
- Voltage source
- Current source
- Magnetic Bias source

Boundaries (from HFSS help)

Boundary conditions specify the field behavior on the surfaces of the problem region and object interfaces. This area of the technical notes includes information about the following boundary types:

- Perfect E
- Perfect H
- Impedance
- Radiation
- PML
- Finite Conductivity
- Symmetry
- Master and Slave
- Lumped RLC
- Layered Impedance
- Infinite Ground Planes

Solution Types (from HFSS help)

- **Driven Modal Solution**

Choose the Driven Modal solution type when you want HFSS to calculate the modal-based S-parameters of passive, high-frequency structures such as microstrip, waveguides, and transmission lines. The S-matrix solutions will be expressed in terms of the incident and reflected powers of waveguide modes.

- **Driven Terminal Solution**

Choose the Driven Terminal solution type when you want HFSS to calculate the terminal-based S-parameters of multi-conductor transmission line ports. The S-matrix solutions will be expressed in terms of terminal voltages and currents.

- **Eigenmode Solution**

Choose the Eigenmode solution type to calculate the eigenmodes, or resonances, of a structure. The Eigenmode solver finds the resonant frequencies of the structure and the fields at those resonant frequencies.

Advantages and Disadvantages of HFSS

The pros and cons of using the HFSS simulator are listed in table below:

Pros	Cons
✓ Large problems can be solved (matrix equations are simple leads to a sparse system matrix) ✓ Arbitrary objects can be ✓ simulated ✓ Automatic mesh refinement ✓ Extremely versatile ✓ Large number of different ✓ excitation/boundary types ✓ Very useful for simulating ✓ periodic structures ✓ User-defined plots ✓ Optimization procedures ✓ Easy to learn and use	✓ Entire volume must be ✓ discretized ✓ Large matrice equations have to be solved (most simulations take too long when using an average PC)

Appendix B

Fabrication Process (Photolithography)

Photolithography is a process that is used for micro fabrication. It plots pattern on parts of thin films or substrate using light to transfer geometric patterns from a photomask to a light-sensitive chemical 'photoresist' material on the substrate. With the process of series of chemical statements, an exposed pattern can be either engraved on the photoresist material or desired pattern can be formed by decomposition of new material. This appendix explains the manufacturing process for fabricating the linear array that has been carried out in the laboratories of D3 building in department of Signal theory and Communications at UPC, using standard techniques of photo plotting.

Block Diagram of Manufacturing Process

The block diagram of the manufacturing process and its description has been listed in this section.

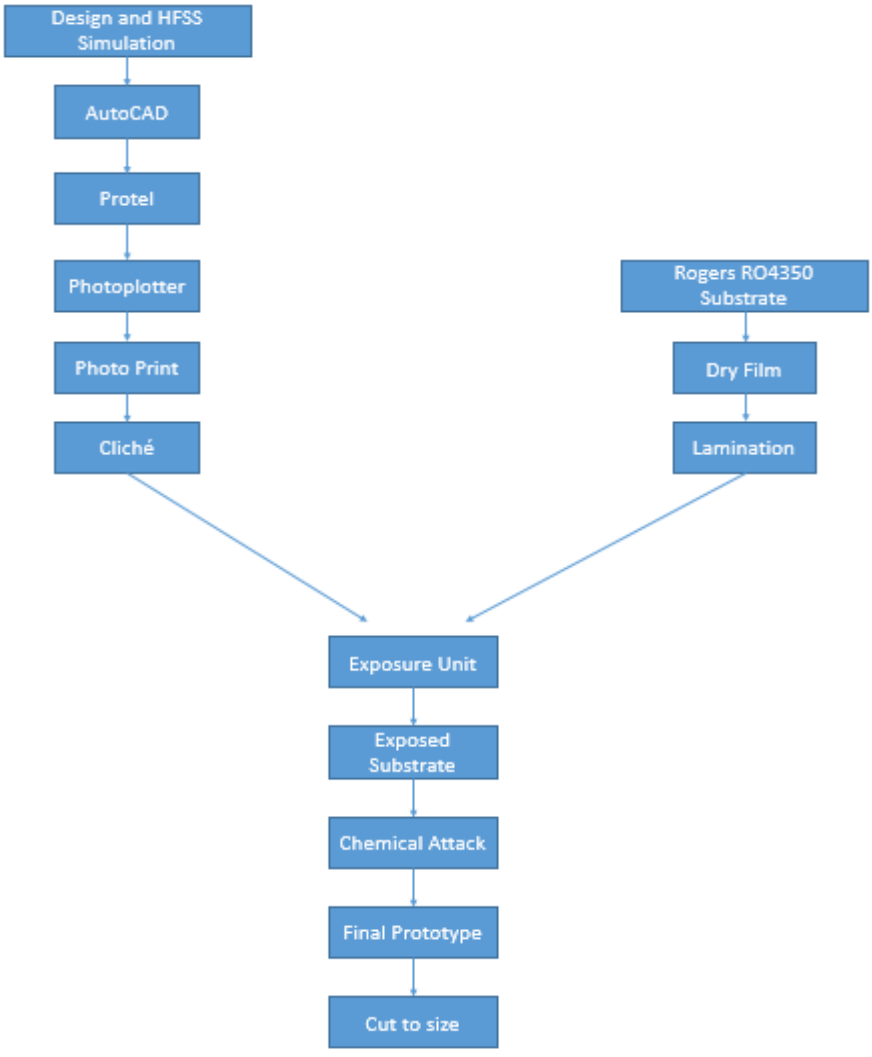

Fig B.1: Block Diagram of the Manufacturing Process Antenna Array using Photolithography

For carrying out the process of photo plotter following three major steps have been performed in the laboratory. Each step includes a number of tasks that are explained as well.

Step 1:

- ✓ Designing and simulated in HFSS the required prototypes.
- ✓ Importing the design geometry into AutoCAD to get an exact measure of the design
- ✓ Importing AutoCAD files to Protel to convert to a format understandable by Photoplotter.
- ✓ Photoplotter prints the design on a film generating high contrast mask.
- ✓ Revealed mask generated by Photoplotter liquid developer and fixer liquid.
- ✓ Obtaining the final cliché (photographic negative).

The whole process of generating the photographic film is done under the security light so that the film is not spoiled.

Step 2:

- ✓ Getting the required substrate for the prototypes (in our case it is Rogers RO4350)
- ✓ Placing a dry film i.e. a photoresist material on to the substrate
- ✓ Fixing the photoresist onto the substrate using lamination

Step 3:

- ✓ The final cliché from the step 1 and dielectric substrate from step 2 are taken and the cliché (containing the geometry of the design) is placed onto the dielectric substrate (with photoresist material on it) in the exposure unit and then is exposed to the ultraviolet light from the machine.
- ✓ The photoresist is fully exposed except for the areas covered by the drawing of the geometry by the photographic film, which allows light to leave the pattern on the substrate. Now we get the exposed substrate
- ✓ A solution of caustic stripper is used that removes the photosensitive resin leaving only the bare copper to be removed. At this time you can correct imperfections that have been caused in minimal parts of the design during the process using a marker to cover parts of copper to protect from chemical attack.
- ✓ A chemical etching is performed which will remove the exposed copper and gives the printed antenna onto the substrate. The chemical etching is done directly with a solution consisting of hydrochloric acid, hydrogen peroxide and water.
- ✓ After the chemical process the designs are rinsed under water and the excess material is removed using cotton and acetone. Now the designs can be further corrected using the microscope and stiletto, and the left over copper can be removed in between the gaps since the gap size is of the order of 150 um.
- ✓ At last the prototypes are cut to the required sides.

Images of the Manufacturing process

Some of the images from the process are shown in this section

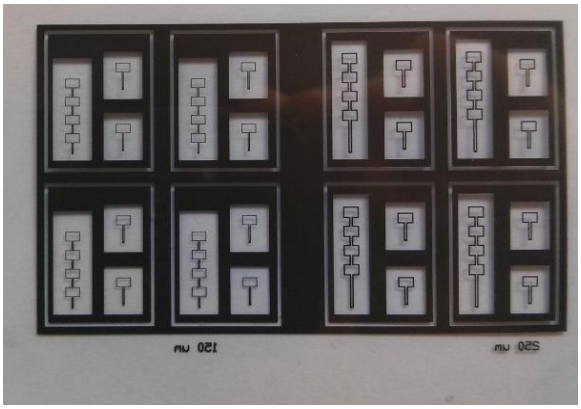

Fig B.2: Final Photographic film with drawing of the geometry (left) and the Mega laminator for laminating dry film (photosensitive resin) onto the substrate (right)

Fig B.3: Substrate after the removal of copper by chemical process (left) and removing the photosensitive material using acetone (right)

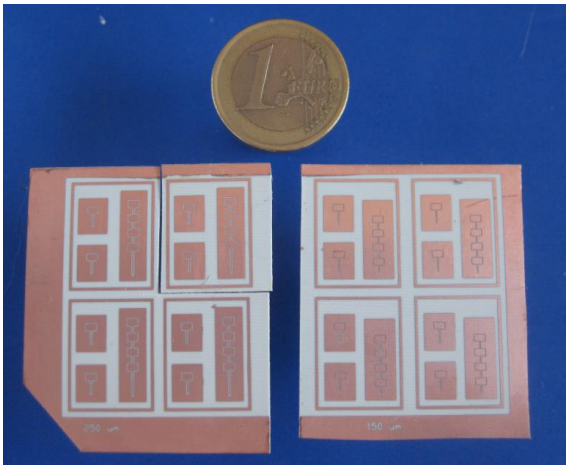

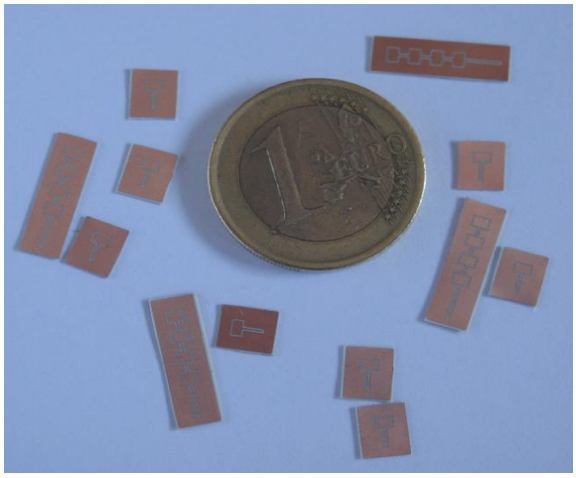

Fig B.1: Substrate film after cleaning with the acetone (left) and separating all the prototypes by cutting (right)

Glossary

BW	Bandwidth
CPW	Coplanar Waveguide
CTTC	Centre Tecnologic Telecommunications Catalunya
ECMA	European Computer Manufacturers Association
FFT	Fast Fourier Transform
FEM	Finite Element Method
GCPW	Grounded Coplanar Waveguide
GSG	Ground-Source-Ground
HFSS	High Frequency Simulator
IC	Integrated Circuit
IEEE	Institute of Electric and Electronics Engineering
LPKF	Laser and Electronics AG Company
MIL	Milli Inch
MMICs	Monolithic Microwave Integrated Circuits
mmW	Millimeter Wave
RF	Radio Frequency
RL	Return Loss
TEM	Transverse Electromagnetic
VNA	Vector Network analyzer
VSWR	Voltage Standing Wave Ratio
WiGig	Wireless Gigabit
WLAN	Wireless Local Area Network
WPAN	Wireless Personal Area Networks